LASER CLADDING OF PURE COPPER POWDER ON MILD STEEL SUBSTRATE WITH CO$_2$ LASER

Submitted in fulfillment of the requirements of the degree of
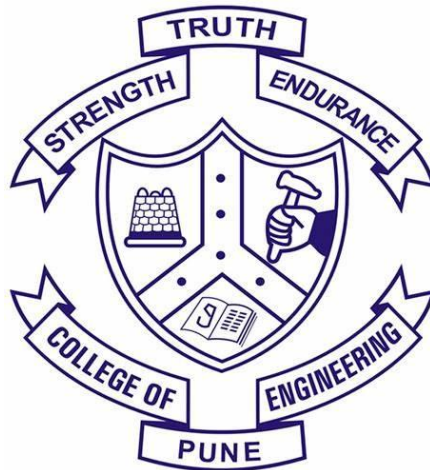
Master of Technology

by

SHUBHAM KAMBLE

(MIS No. 122046006)
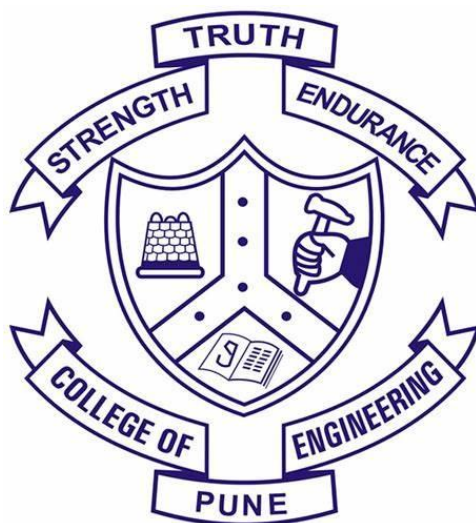
Under Guidance of:

Prof. M.J. Rathod

Department of Metallurgy and Materials Science

COLLEGE OF ENGINEERING PUNE

(JAN, 2023)

CERTIFICATE

This is to certify that the report entitled **'Laser Cladding of Pure Copper Powder on Mild Steel Substrate with CO$_2$ Laser'** submitted by **Mr. Shubham Kamble** (MIS No: **122046006**), in the partial fulfillment of the requirement for the award of degree of Master of Technology (Department of Metallurgy) with specialization in **Materials Engineering** of College of Engineering Pune, affiliated to the Savitribai Phule Pune University, is a record of his own work.

Prof. M.J. Rathod   **Dr. S.P. Butee**

Guide   **Head of the Department**

Department of Metallurgy   **Department of Metallurgy**

and Materials Science   **and Materials Science**

College of Engineering, Pune   **College of Engineering, Pune**

Date:

Place:

APPROVAL SHEET

This report entitled

Laser Cladding of Pure Copper Powder on Mild Steel Substrate with CO_2 Laser

by

SHUBHAM KAMBLE

(MIS No: 122046006)

is approved for the degree of

Master of Technology with specialization in Materials Engineering

of

Department of Metallurgy and Materials Science

College of Engineering Pune

(An autonomous institute of Govt. of Maharashtra)

Examiners	Name	Signature
1. External Examiner	_____	
2. Internal Examiner	_____	
3. Supervisor (s)	_____	

Date:

Place:

Declaration

I declare that this written submission represents my ideas in my own words and where others' ideas or words have been included, I have adequately cited and referenced the original sources. I also declare that I have adhered to all principles of academic honesty and integrity and have not misrepresented or fabricated or falsified any idea/data/fact/source in my submission. I understand that any violation of the above will be cause for disciplinary action by the Institute and can also evoke penal action from the sources which have thus not been properly cited or from whom proper permission has not been taken when needed.

_____

(Signature)

SHUBHAM KAMBLE

(Name of the student)

122046006

(MIS No.)

Date:

Place:

LIST OF FIGURES

LIST OF TABLES

ABSTRACT

Laser cladding was performed to improve the surface properties of the metallic machine parts generally. Bonding material with desirable properties is laser cladded onto the substrate using a laser beam. Mixing/Dilution between two materials should be as small as possible in order to take the advantage of the coating materials effectively. By improving the surface properties in the area of dedicated materials, one can use low cost base material which is not exposed to severe working conditions. Laser cladding results in superior properties in terms of purity, homogeneity, hardness, bonding and microstructure.

In this work, laser cladding of copper powder on mild steel substrate is performed with variation in parameters like laser power (power density), scan speed, hatch spacing, direction of scanning and number of layers. Effect of these parameters was studied on hardness, bond shear strength, density, porosity and microstructure. The copper powder was characterized for particle-size, apparent density and flow rate.

Under the condition of horizontal scanning, power 140 w, scan speed 13 mm/sec, hatch space 0.5mm, the cladded specimen showed peak hardness of 125.32 HV, shear load of 23.6 kN and secondary dendritic arm spacing (SDAS) of 8.90µm.

TABLE OF CONTENTS

CHAPTER 1

INTRODUCTION

In industries such as aerospace, Petro-chemistry, and automotive, many parts of the various machinery in nature are exposed to high temperatures and high pressures, which causes them to age and rust [1]. Therefore, wear resistance and stability under high temperatures require continuous improvement. At the moment, Laser cladding (LC) is widely used in machine parts repair due to its advantages such as low cleaning rate, low heat-affected area, and good metallurgical bonding between coating and substrate.

The laser-cladding technique can provide a very promising way to restore the geometry and structural integrity of carbon steel parts affected by corrosion cracks and wear damage. This feature of laser cladding makes it one of the most promising ways to transform the environment [2]. The laser-cladding layer with fine metallurgical bonding and substrate is made using high-energy laser density to dissolve metal powders. The extra performance is enhanced by conveying a laser-cladding layer with very high aging and corrosion resistance. Compared to other surface area conversion techniques, such as spray coverage, electroplating, vapor deposition, etc., laser cladding requires low cleaning and can produce a layer with good microstructure and good adhesion to the substrate, leading to its widespread use in aerospace, mold, and electronics industries.

Carbon metals are the most widely used engineering material due to their availability, structure, and modest cost [3]. However, carbon steel delivers a limited-service life due to its poor corrosion resistance. One way to improve the surface properties of carbon steel is to apply a coating of corrosion-resistant materials such as stainless steel using a laser cladding process. Which provides many advantages like low cost, high corrosion resistance, high strength and weldability of carbon steel.

Surface modification methods like Laser cladding and surface alloying are used to create a thin layer or coating which improves the surface properties or restores the surface defects by providing a highly resistant coating or layer on the substrate [4]. High power density and high cooling rates make these methods suitable for the wide scope width of materials. In recent years, due to the development of high-power lasers, improved control and Delivery methods have attracted in-depth research into laser surface treatment. Researchers have analysed the various aspects of processes to improve process performance. Experimental research and

theory show that the effectiveness of laser cladding and surface alloying techniques can be greatly improved by the proper selection of the laser process parameters.

Copper has unique features like thermal conductivity, electrical conductivity and friction characteristics, it has been anticipated that copper will form films on engineering components as a surface treatment material [5]. Many techniques have been used, including arc welding, thermal spraying, plasma-transferred arc welding, and others, to generate coating on the surface of components. However, these techniques frequently resulted in issues with low adherence and significant dilution between a substrate and a coated film. Due to the laser's excellent heat controllability, the laser cladding process has recently been employed extensively to generate functional films on substrates with controlled heat input.

In this work, pure copper powder was selected as a cladding material on a mild steel substrate, for which the experimentation was performed by varying the process parameters like laser power density, scanning speed, hatch space, scanning strategy, and also a number of layers with an objective to get an optimum process parameters. The effects of changing the process parameters were compared based on layer hardness, bond shear strength, secondary dendritic arm spacing (SDAS), layer density, and porosity.

This work involves microstructural analysis, and mechanical testing of laser cladded samples using copper powder on a mild steel substrate. Based on the experimentation, the optimum process parameters were obtained.

CHAPTER 2
LITERATURE REVIEW

There are many different additive manufacturing processes available. The key variations across procedures are how layers are deposited to generate pieces and the raw material being processed. Powder preparation, compaction, and the time-consuming sintering process are all steps in the traditional powder metallurgy manufacturing process. As a result, today's layer-by-layer printing of metals is being developed using a novel technique called additive manufacturing (AM). The substance utilized may be either liquid or solid.

2.1 Additive Manufacturing

AM is a cutting-edge technique that uses data from Computer-Aided Design (CAD) to automatically create physical models. It is layer-by-layer manufacturing technology [6]. Rapid prototyping procedures often start with a three-dimensional computer model of the intended component. Computer software slices this digital image of the part into virtual layers. The RP machine receives each layer, which represents a cross-section of the desired part, and builds on the layer before it.

Rapid prototyping processes build the part in layer-by-layer form. This process is repeated until the part is completed as shown in Fig. 2.1. Rapid prototyping systems can produce models from 3D CAD data, CT and MRI scans, as well as 3D digitizing systems. Using an additive approach, rapid prototyping systems join liquid, powder, or sheet materials to form physical objects on a layer-by-layer basis [6]. Rapid prototyping machines process plastic, paper, ceramic, metal, and composite materials from thin, horizontal cross-sections of computer models.

Additive manufacturing (AM) consists of the following steps:

1. Develop a computerized 3D model of the required shape [7].

2. Convert it into AM standard file format to prepare G-Codes of every layer.

3. Send a file to AM machine for manipulation.

4. Build part on AM machine layer by layer.

5. Clean and finish the 3D sintered model.

Additive manufacturing creates "things" from a digital model by layer-by-layer depositing the constituent elements with the use of material laying equipment that are digitally controlled

and managed This more inclusive definition of additive manufacturing primarily emphasizes four key elements

AM CATEGORY	Vat Photo-polymersation	Material Extrusion	Material Jetting	Binder Jetting	Power Bed Fusion	Direct Energy Deposition	Sheet Lamination
TECHNOLOGIES	Stereolithography (SLA)	Fused Deposition Modeling (FDM) Contour Crafting	Polyjet / Inkjet Printing	Indirect Inkjet Printing (Binder 3DP)	Selective Laser Sintering (SLS) Direct Metal Laser Sintering (DMLS) Selective Laser Melting (SLM) Electron Beam Melting (EBM)	Laser Engineered Net Shaping (LENS) Electronic Beam Welding (EBW)	Laminated Object Manufacturing (LOM)
MATERIAL	Photopolymer Ceramics	Thermoplastics, Ceramic slurries, Metal pastes	Photopolymer, Wax	Polymer-, Metal- or Ceramic powder	Polymer-, Metal- or Ceramic powder	Metal powder or wire	Plastic film, Metallic sheet, Ceramic tape
PROS/CONS	+ High building speed + Good part resolution – Overcuring, scanned line shape – High cost for supplies and materials	– Inexpensive extrusion machine – Multi-material printing – Limited part resolution – Poor surface finish	+ Multi-material printing + High surface finish – Low-strength material	+ Full-color + Wide material selection – Require infiltration during post-processing – High porosities on finished parts	+ High Accuracy and Details + Fully dense parts + High specific strength & stiffness – Powder handling & recycling – Support and anchor structure	+ Repair of damaged/worn parts + Functionality graded material printing – Bad resolution – Expensive	+ High surface finish + Low cost – Decubing issues

Fig 2.1. An overview of AM technologies [7].

- A digital representation of the item, which may be anything from a screw to an airplane wing.
- Materials that are combined in the tiniest form possible, such as liquid droplets, wire, and powder, to create the thing.
- A tool for layer-by-layer material application
- A digital control system is required to construct the shape of the object.

Some of the potential benefits of additive manufacturing can be summarized below:
- Directly converting a design into a component
- Functional design that enables the production of intricate internal features
- Manufacturing of flexible and lightweight components using lattice or hollow structures.

- Possibility of achieving zero waste manufacturing by optimizing material utilization.
- Reduced operational footprint for producing a wide range of parts.
- On-demand production, an alternative to manufacturing based on projections.
- Outstanding scalability.

2.2 Additive Manufacturing Processes

Different layer-building and layer-consolidation techniques are used in additive manufacturing. Laser or electron beam thermal energy is used in some operations [8]. In order to generate a coherent mass without melting metal or plastic powder together, it is directed by optics to melt or sinter. In other procedures, binder or solvent are precisely sprayed onto powdered ceramic or polymer using printing heads similar to inkjets. The two main categories of metal additive manufacturing (AM) methods are those based on powder bed fusion (PBF) and those based on directed energy deposition (DED). Based on the kind of energy source employed, both of these technologies can be further categorized.
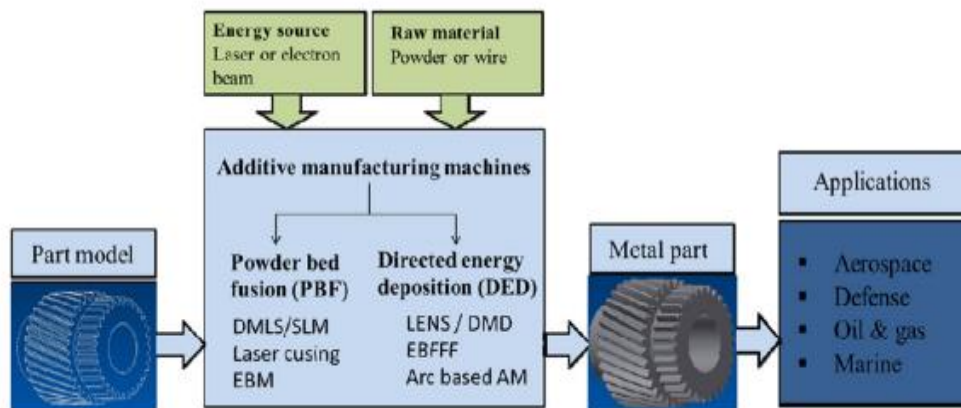
Fig.2.2 Common metal additive manufacturing process [8].

2.2.1 Powder-based fusion (PBF)

The most typical techniques of Powder based fusion technologies are selective laser sintering (SLS) selective laser melting (SLM), direct metal laser sintering (DMLS), and electron beam melting (EBM), which use heat energy to specifically fuse portions of the powder [8]. Powder-based fusion method, DMLS sinters components together using metal powder and a strong laser. Although this process can provide very dense parts, post-treatment is frequently needed to achieve gas or pressure tightness. The procedure is fundamentally the same as selective laser sintering (SLS), an existing additive manufacturing technique, except in DMLS, the sintering material is uncoated pre-alloyed metal powders rather than polymers or

coated metal powders, as in SLS. With the help of an electron beam energy source similar to that used in electron beam welding, a heated metal powder bed is melted and built up layer by layer using the electron beam melting (EBM) technique.
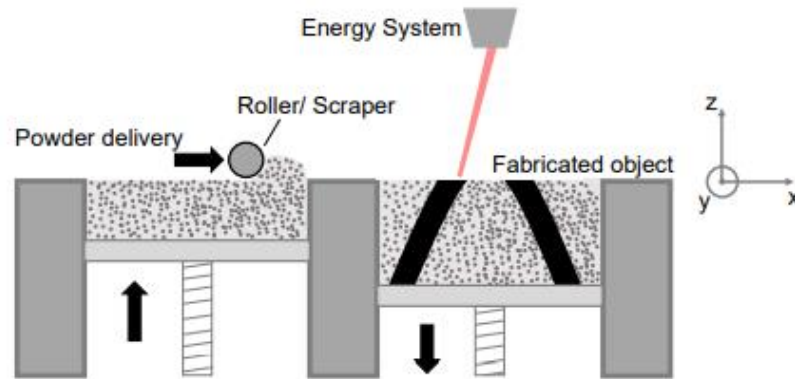
Fig 2.3. Overview of the Powder Bed Fusion manufacturing process [8].

2.2.2 Laser Cladding

LASER cladding is regarded as a surface-treatment method. With LASER, three categories of surface treatment methods can be separated [9]. The group of techniques with surface hardening (or without surface melting), the group of techniques with surface melting, and the group of techniques with surface melting and with additional material. It becomes required or more cost-effective to apply a layer of another material to the base material's surface if the base material is unable to increase its mechanical characteristics on its own using melting or hardening procedures.

LASER cladding is a technology that, in addition to its further use in the production of 3D components, has as its primary goal, as already said, improving the mechanical characteristics of materials surface through the addition of thin layers of various materials [9]. When a thin layer of a particular material with desirable qualities is deposited on a particular substrate using LASER as the heat source, the cladding material's surface and the substrate's surface melt, resulting in LASER cladding. The absorption of energy from the LASER beam heats the region that will be covered. A high-power LASER beam's heat input is tightly focused and extremely intense (the most common power in industrial applications is above 5 kW), which accelerates the heating of the surface layer. Following the passage of the LASER, the heated top layer is quenched as a result of heat being transferred to the bulk's coldest region. High rates of heating and cooling in the surface layer cause the microstructure to change, metastable phases to arise, and grain refinement. The CO2 LASER and other Nd: YAG

LASER types have traditionally been used in the LASER cladding process, but more recently, the usage of fibre LASER has been favored.

In addition to the method of pre-placing the material's powders on the substrate, cladding material can also be applied to the substrate continuously during the cladding process via wire feeding, powder injection, or paste feeding. Next, a scheme for the two LASER cladding techniques is shown in Fig. 2.4.
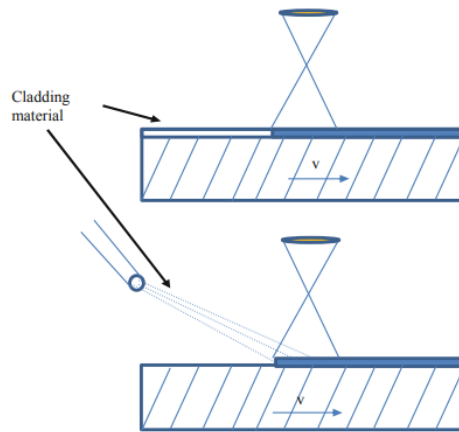
Fig.2.4 Schematic of LASER cladding executed by the pre-placed powder method (top part) and by the powder injection method (bottom part) that corresponds to one of the variants of the continuous material feeding method. A LASER beam reaching the material is schematized and the dislocation direction of the substrate is represented by v [9].

2.2.3 Pre-Placed Powder Method

The pre-placed powder method is a two-step process that starts with applying powder to the substrate in the first stage [9]. To ensure a strong binding between the cladding material and the substrate while the procedure is carried out, the powder should be combined with a chemical binder and spread throughout the substrate as a paste. Some porosities in the clad layer may be the result of the binder evaporating throughout the process. The second stage sees the development of a melt pool on the cladding material's surface, which later spreads to the substrate contact. After heating, it is feasible to extend the melt pool onto the substrate, forging a solid bond between the newly added material and the substrate.

In Laser Cladding, there is a clear difference between coating and substrate with a low layer distribution layer. Also, the coating provides a covering of the substrate and shows more structures of only worn items [4].
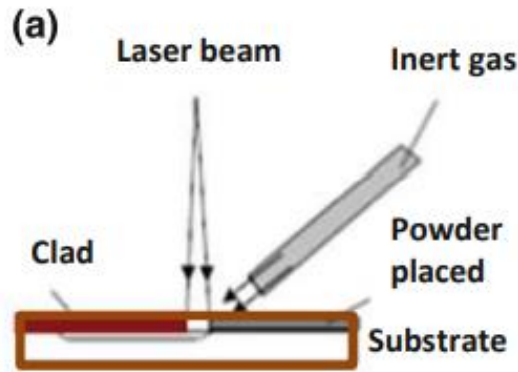
Fig.2.5 Schematic of the pre-placed powder method [9].

2.3 Selective Laser Sintering Technology

Selective Laser Sintering is a process that was patented in 1989 by Carl Deckard. Selective laser sintering was first done mainly on polymers and nylon to create prototypes [6]. It was expanded to include metals and alloys to manufacture functional prototypes and develop rapid tooling. The selective laser sintering (SLS) process now stands as an alternative to conventional manufacturing techniques due to its varied material capabilities.
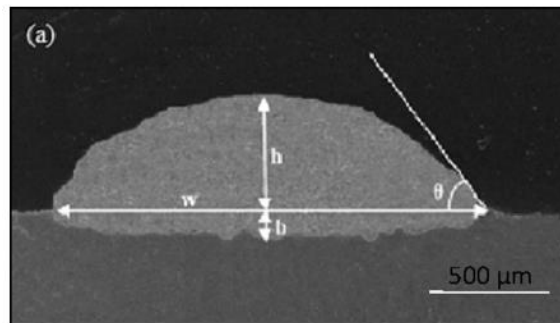
Fig.2.6 SEM cross-sectional images of laser clad coating [4].

Selective laser sintering can process a wide range of materials hence; it is superior to other rapid manufacturing techniques. The term 'sintering' refers to a process by which objects are created from powders using the mechanism of atomic diffusion. Atomic diffusion occurs in any material above absolute zero and the process occurs much faster at higher temperatures hence sintering involves heating a powder. Sintering is different from melting. In that, materials never reach to a liquid phase during the sintering process.
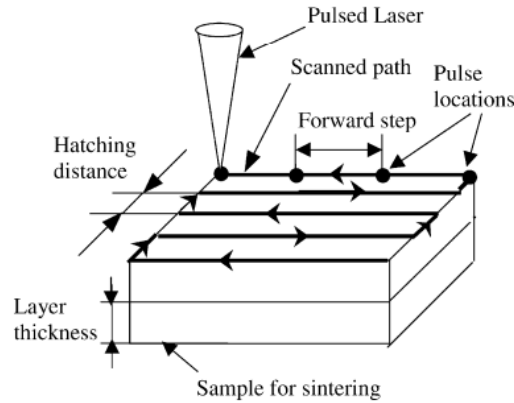
Fig.2.7 SLS system [6]

The selective laser sintering system and its terminology are shown in Fig.2.13 and Fig.2.14 respectively. It is a powder-based layer additive manufacturing process generally meant for rapid prototyping and rapid tooling. In continuous or pulse mode, laser beam is used as a heat source for scanning and joining powders in a predetermined size and shape of layers. The geometry of the scanned layers corresponds to the various cross-sections of the computer-aided design (CAD) models or (STL) files of the object. After the first layer is scanned, a second layer of loose powder is deposited over it and the process is repeated from bottom to top until the part is complete. In this process, a high-power laser beam selectively melts and fuses powdered material spread on a layer[7]. The powder is spread by a powder spreader on the table in a precise amount. A laser beam is used to fuse the powder within the section boundary through a cross-hatching motion. The table is lowered through a distance corresponding to the powder layer thickness before the roller spreads the next layer of powder on the previously built layer. The not sintered powder serves as the support for overhanging portions if any in the subsequent layers [6].

2.3.1 Sintering Mechanism

As shown in Fig.2.15, it shows the process by which powder particles sinter [8]. It consists of diffusion mechanisms including grain boundary diffusion, surface diffusion, lattice diffusion, and vapour transport. It is the process of compacting either a green compact with the desired composition or a loose aggregation of powder under controlled temperature and time conditions. Heat treatment is used in the sintering process in Fig.2.13 SLS system [7] and Fig.2.14 SLS terminology [7], which bonds the metallic particles and increases strength and hardness. Sintering typically takes place at temperatures between 70% and 90% of the metal's melting point.
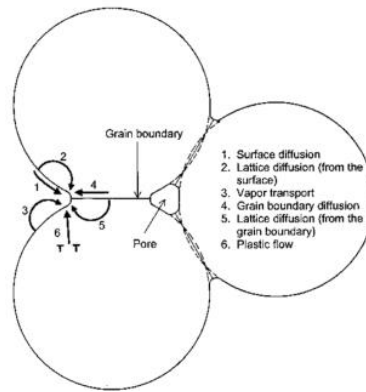
Fig.2.8 Sintering Mechanism [8].

A. Solid-state sintering
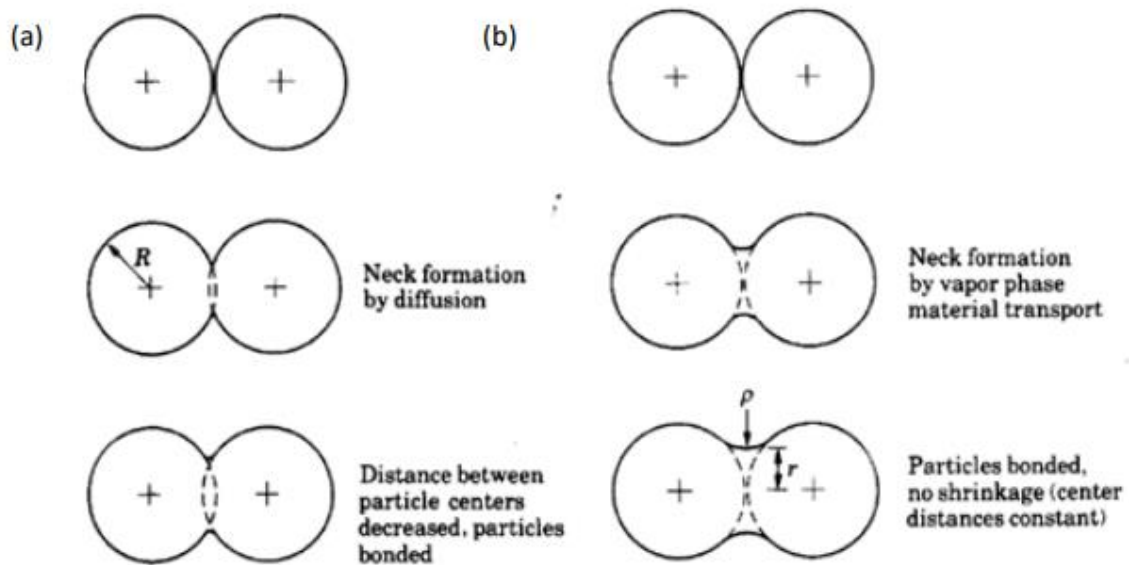
Fig.2.9 Schematic illustration of two mechanisms a) solid state sintering
b) liquid state sintering of metal powder.

Solid-state sintering is depicted in Fig. 2.9 (a). Atomic diffusion occurs during this type of sintering [8]. Diffusion could take the form of boundary, surface, or volume diffusion. The creation of a neck at the boundary of two powder particles results from diffusion. When the neck is expanded, more diffusion fills the space and binds the powder particles. A sufficient temperature and time must be present for diffusion to occur. Since melting of the powder would prevent solid-state sintering, there is rigorous control over the process parameter.

B. Liquid phase sintering

Figure 2.18 (b) depicts the sintering of metal powder in the liquid state, which is the most frequent mechanism in laser sintering [7,8]. Surface melting and connecting of a non-melted

particle core occurs in single-component powder systems via a liquid bridge. In order to achieve solely surface melting of particles, strict parameter control is therefore necessary. One of the components with a lower melting point in a multi-component powder system partially or completely melts.

As a result, it creates a liquid phase and binds other substances with greater melting points. Melting occurs in a pre-alloyed powder system over the range of temperatures between solidus and liquidus temperatures. A liquid phase can occur during laser sintering depending on the temperature, creating a mixture of solid and liquid that results in super-solidus sintering.

C. Chemical-induced bonding

The bonding of particles occurs as a result of a chemical process that occurs during laser-material interaction [10]. For instance, SiC powder separates into Silicon (Si) and Carbon (C) when scanned by a laser. Si then undergoes a reaction with oxygen gas to produce SiO2, a compound with a low melting point. Sintering results from the binding of the residual SiC particles by molten SiO2. Figure 2.17 illustrates the various binding methods used for laser sintering and laser melting of several kinds of powder systems. Partial melting/liquid phase sintering makes up the majority of the binding mechanism in laser sintering. In laser melting, the binding mechanism completely melts and then solidifies. Chemically induced binding in laser sintering is a rare mechanism. C and Si then undergo a reaction with oxygen gas to produce SiO2, a compound with a low melting point. Sintering results from the binding of the residual SiC particles by molten SiO2. Figure 2.17 illustrates the various binding processes for laser sintering and laser melting for several kinds of powder systems. Partial melting/liquid phase sintering makes up the majority of the binding mechanism in laser sintering. The binding mechanism is completely melted during laser melting, and then solidification follows. Chemically induced binding in laser sintering is a rare mechanism.

2.4 Laser as a heat source

The acronym for "light amplification by stimulated emission of radiation" is "LASER." Schawlow and Townes had first put out the idea. With the help of optical amplification and stimulated emission, a laser emits light [11]. It is discovered that the stimulated photons are moving in the same direction and are in phase with the stimulating photons. The energy transition between an excited state and a lower state gives rise to a photon. Due to population inversion and stimulated emission, photons are released.

The fundamental reason why lasers are used in various industries for a variety of applications is because of their properties. Lasers have the following characteristics: directionality, minimal divergence, high intensity, high coherence, and high monochromaticity. Gas lasers, chemical lasers, excimer lasers, solid-state lasers, fiber lasers, semiconductor lasers, dye lasers, and free-electron lasers are some of the laser types that are now accessible. Different output powers of lasers are required for various applications. The average power of lasers that emit a continuous beam or a succession of brief pulses can be compared. The peak power of each pulse from pulse-producing lasers can also be used to describe them.

a) Basic components of Laser

The laser consists of three basic components [12]

1. Active medium: - In active medium amplification of light takes place. It can be in form of solid, liquid, gas, and plasma.

2. Pumping source: -Pumping source is used to excite the active medium to the amplifying state. The common pumping source includes flash lamps, lasers, electrons, chemical reactions, ion beams and X-ray sources.

3. Optical resonator: - It is used to provide optical feedback. An optical resonator is a cavity, defined by 100 % reflective mirror at one end and a partially transmitting mirror at another end.

b) Types of Laser

The energy difference as the excited species is stimulated to a lower energy level determines the wavelength of the laser[11,12]. In general, quantum states refer to ionization effects with ultraviolet lasers, electron orbit levels with visible laser radiation, and molecular vibration levels with long-wavelength lasers. The most widely used systems for material processing are CO2, Nd: YAG, and fibre lasers. Diode and excimer lasers are also quickly entering the market. There are numerous varieties of lasers. A semiconductor, gas, liquid, or solid can be the laser medium. The sort of lasing material used to create a laser is a typical way to identify them.

1. Gas Lasers

The light-amplifying material in gas lasers is a gas or a combination of gases. The most popular gas lasers are helium-neon, argon ion, and carbon dioxide lasers. The gases can be adjusted to alter the output wavelength. The carbon dioxide, carbon monoxide, and excimer lasers make up the gas laser.

2. Solid-state Lasers

The active medium in solid-state lasers is enclosed in an insulating dielectric crystal made of amorphous glass[11]. The transition between distinct electronic energy levels of the dopant, such as rare earth ions or transition ions with empty outer shells or defect centers known as colour centers, is what causes the lasing activity. Nd3+:YAG, Er3+:YAG, Yb3+:YAG, ruby (Cr3+:Al2O3), titanium sapphire (Ti3+:Al2O3), and alexandrite (Cr3+:BeAl2O4) are the primary industrial solid state lasers. The advantage of relatively extended excited state lifetimes for solid-state lasers. Compared to gas lasers, it enables increased energy storage, allowing them to be Q-switched to produce very high peak outputs in brief pulses. Nd-YAG lasers, Neodymium glass lasers, Diode-pumped solid-state lasers, Disc lasers, Fibre lasers, and Semiconductor lasers are a few examples of solid state lasers.

3. Fibre Lasers

Fibre lasers easily dissipate thermal energy and do not lose alignment. These are strong and compact. The fibre laser is a variant of the common solid-state laser, using fibre as the medium as depicted in Fig. 2.18. They come in a variety of shapes and sizes, sharing technology with other kinds of lasers but offering their own special benefits. Doping in the fiber's central core causes the emission of laser light. Diode lasers pump the ends or sides of doped glass fibres to create these lasers[12]. Erbium and Ytterbium, two rare earth elements, are doped in silica glass fibre. Because they have useful energy levels, rare earth elements are used. A key factor for fibre laser is that the fibre has a large surface-to-volume ratio so that heat can be dissipated easily.

2.4.1 Laser beam characteristics

The use of a laser for various applications depends upon the beam properties of the laser, such as direction, divergence, and wavelength or frequency characteristics, which can be adjusted by the laser components[13]. The features affecting the beam properties of laser include size of the gain medium, location, separation and reflectivity of the mirrors of the optical cavity, and presence of losses in the beam path within the cavity. Some of these features determine the unique properties of the laser beam, referred to as laser modes[10]. The laser modes are wavelike properties relating to the oscillating character of the beam as the beam passes back and forth through the amplifier and grows at the expense of existing losses. The development of laser modes involves an attempt by competing for light beams of similar wavelengths to fit an exact number of their waves into the optical cavity.

a. Wavelength

The wavelength depends on the transitions taking place by stimulated emission. The wavelength may be broadened by Doppler effects due to the motion of the emitting molecules or by related transitions from higher quantized states.[13]

b. Coherence

The stimulated emission phenomenon means that the radiation is generating itself and in consequence, a continuous waveform is possible with low-order mode beams [9]. The length of the continuous wave train may be many meters long. This long coherence length allows some extraordinary interference effects with laser light.

c. Polarisation

The stimulated emission phenomenon not only produces long trains of waves but these waves will also have their electric vectors all lined up. The beam is thus polarised. The beam is thus polarised. Many of the early lasers and some of the more modern ones which do not have a fold in the cavity will produce randomly polarised beams.

d. Laser beam quality- M^2 factor

The ratio of divergence of actual beam to the theoretical diffraction-limited beam is known as M^2 factor [12]. Beam quality is measured with M^2 or $1/k$. Ideal Gaussian beam has M^2 value of this beam is perfectly diffraction limited. This factor allows higher order mode in a laser beam. The factor M2 can be determined by eq^n [14].

$$M^2 = \frac{1}{k} = \theta \times \frac{\pi\,Do}{4}\,\lambda \qquad \ldots\ldots\ldots\ldots\ldots\ldots \text{Eq.}(2.1)$$

Where,

Do = Diameter of natural beam

θ = Angle of divergence of beam

λ = Wavelength of the corresponding beam.

e. Beam diameter focusing

Beam diameter can be focused with the use of optical lenses. When a continuous beam with a constant diameter is fallen on an optical lens then it is converted into a focusing point. It means its cross-sectional diameter gets changed. It gives different beam diameters at different focusing distances as shown in Fig.2.22.

f. Surface temperature

The surface temperature developed by laser at any time, t, after the start of irradiation is given by equation[14].
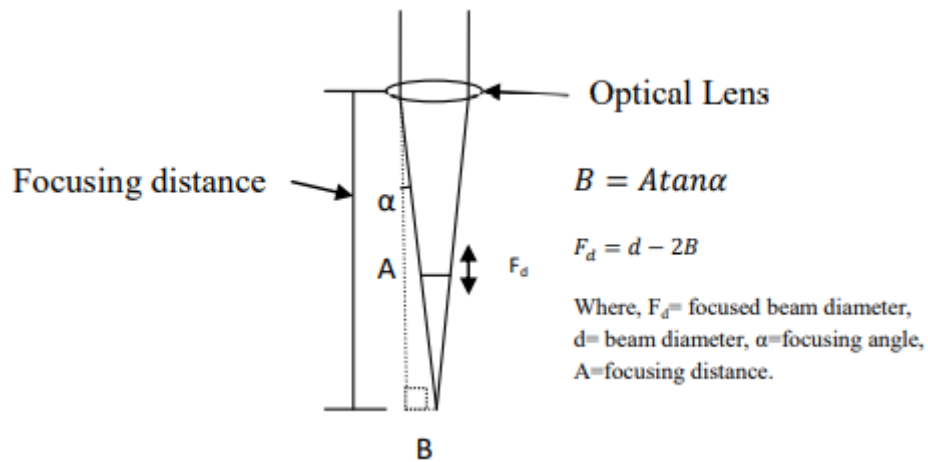
Fig.2.10 Focused diameter Fd changes with focusing distance [12].

$$T(0, t) = \left(\frac{2Fo}{K}\right)\left[\frac{(\alpha t)}{\pi}\right]^{1/2} \qquad \ldots \ldots \ldots \ldots \ldots \ldots \text{Eq.(2.2)}$$

Where,

Fo= Power density, W/m^2

K=Thermal Conductivity, W/mk

t=interaction time, S

α=thermal diffusivity, m^2/s

g. Absorption and Reflection of laser beam

The value of the absorption coefficient will vary with the same effects that affect the reflectivity [14].

For opaque materials,

   Reflectivity = 1 − absorptivity

For transparent materials,

   Reflectivity = 1 − (transmissivity + absorptivity)

In metals, radiations are absorbed by free electrons. These free electrons are free to oscillate and re-radiate without disturbing the solid atomic structure. Thus, reflectivity of metal is very high. As a wavefront arrives at surface, then all the free electrons in the surface vibrate in phase, generating an electric field 180⁰ out of phase with the incoming beam. The sum of this

field will be a beam whose angle of reflection equals the angle of incidence. This "electron gas" within the metal structure means that the radiation is unable to penetrate metals to any significant depth, only one to two atomic diameters. Metals are thus opaque and appear shiny. Absorption is more in metallic powder due to highly interconnected particle reflections. Therefore, more heat is absorbed in powder than in metal plates. As the temperature of the structure rises, there will be an increase in the phonon population, causing more phonon electron energy exchanges. Thus, the electrons are more likely to interact with the structure rather than oscillate and re-radiate. There is thus a fall in the reflectivity and an increase in the absorptivity with a rise in temperature for some metals. Roughness has a large effect on absorption owing to the multiple reflections in the undulations. There may also be some "stimulated absorption" due to beam interference with sideways-reflected beams provided the roughness is less than the beam wavelength, the radiation will not suffer these events and hence will perceive the surface as flat. The reflected phase front from a rough surface, formed from the Huygens wavelets, will no longer be the same as the incident beam and will spread in all directions as a diffuse reflection. It is interesting to note that it should not be possible to see the point of incidence of a red He–Ne beam on a mirror surface if the mirror is perfect.

h. Plasma effect

During the laser sintering with high energy density, more energy is added to the powder, so that melt temperature increases due to which evaporation of some material from irradiated area [15]. There evaporated material interacts with the laser beam and ionization of ions, atoms and molecules. These ionized ions molecule appears in or around the laser beam as plasma. The plasma produced during the laser sintering is undesired during laser sintering because plasma interacts with laser beam and scatters the laser beam and reduce the intensity of the laser beam.

2.4.2 Laser type selection

Many factors are considered during the selection of Laser Surface Treatment procedures [16]. Some of the desirable features are presented in the flow chart shown in Fig.1.4. The material to be considered is one of the factors of laser type selection Sensitive to heat and refractory materials used materials are usually treated in pulsed mode. It is the same again realized that a strong formation of priorities may be different in the case of laser continuous pulse methods. Figure 1.5 indicates the relationship between the appearance of the metal and the wavelength of radiation. Materials, for example, aluminium, with a low alloy absorption,

are usually processed with a small wavelength. Also, desirable structures primarily influence the choice of laser in a particular system.
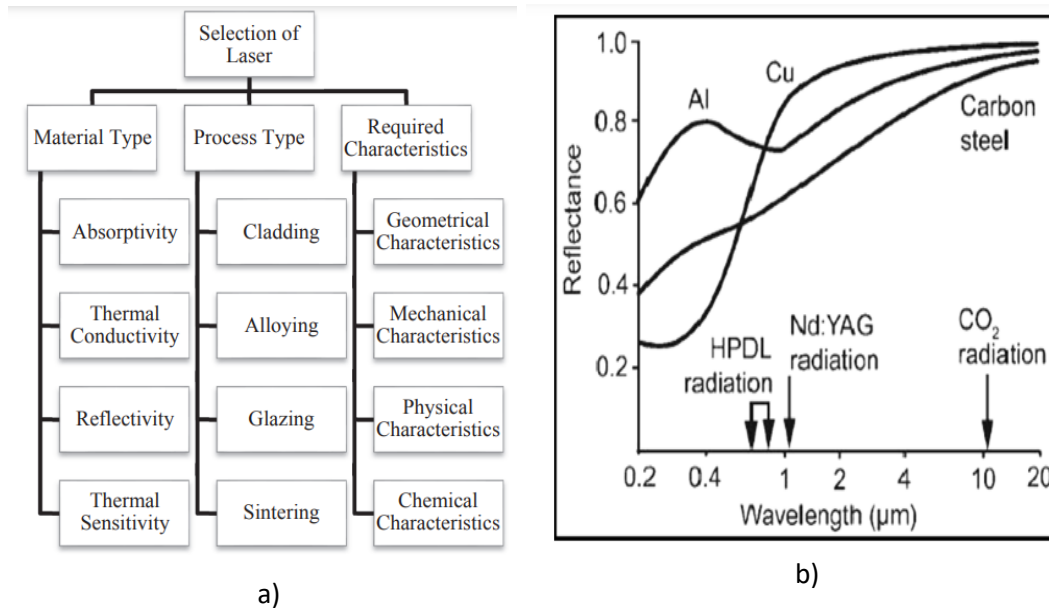

a)

b)

Fig.2.11 a) Critical parameters for choice of laser source type. b) The reflectance Vs. the radiation wavelength of materials[16].

2.4.3 Process Parameters

The parameters that vary in laser cladding include powder size, scan speed, powder density, pulse frequency, scan size, scan spacing, part-bed temperature, layer thickness, pulse size, laser power, laser energy, spot size, powder size distribution, ratio of the powders of the mixture [17] .The design of experiment is necessary to find the significant parameters and the effect of those parameters on the physical and mechanical characteristics of the parts.

a) **Powder density**

Power density is calculated from laser power and beam diameter. It gives how much power is given to c/s area of beam diameter shown in eqn.

$$Pd = \frac{P}{A} \qquad \dots \dots \dots \dots \dots \dots \text{Eq.(2.3)}$$

Where Pd = Power Density (W/mm^2), P= Laser Power (W)

A= Cross-sectional area of beam (mm^2).

b) **Interaction Time:**

It is calculated by using eqn

$$T = \frac{d}{S} \qquad \dots \dots \dots \dots \dots \dots \text{Eq.(2.4)}$$

16

Where T= Interaction time (S)

d= laser beam diameter (mm),

S= Scanning speed mm/s.

2.5 Materials utilized for Laser cladding

There are already a large number of materials that can be used as base materials a process in which various grades of steel, cast iron and non-ferrous metals are involved metals such as nickel, titanium and aluminum alloys. Relative to saved materials on the base material there is also already a large number of metals and the use of metal alloys (mainly hard alloys based on nickel, cobalt and iron), as well as a large number of their compositions[11].

For the base material different groups of metals include the Fe-based materials group including carbon-manganese steels, alloy steels, stainless steels, tool steels and cast irons, the cast and wrought aluminium alloys group, the group of Ni-based superalloys strengthened in the cast and wrought form, the titanium and its alloys group, the magnesium alloys group and the cooper (wrought and cast) and its alloys group.

Whereas for cladding material the Co-based hardfacing alloys group, the Ni-based alloys group, the Fe-based materials group namely, stainless steels, tool steels and Fe-based hard-facing alloys, the Cu-based alloys group, the Al-based coatings group, the Ti-based coatings group and also the group of metallic matrix composites, the group of functionally graded materials, the group of solid lubricants, the group of rare-earth element additions and the group of intermetallics are tested.

2.6 Advantages and limitations of Laser cladding

a) Advantages of Laser cladding

1. Variety of materials can be cladded based on their applications by using Selective laser sintering technology.
2. Material properties like wear and corrosion resistance of base metal can be improved with cladding.[18]
3. Laser cladding is also advantageous when it is utilized as a repair technique.
4. Due to the layer-by-layer production technique it can achieve homogenous structure and good mechanical properties[19].
5. It can be used as an alternative for most of the welding processes that produce high temperatures during a repair.

6. As the laser is used as a heat source it can achieve fine microstructure due to high heating and cooling rates.

7. Mainly in the case of powder injection methods minimum dilution of a substrate, strong fusion bond between substrate and cladding, lesser porosities achieve a homogenous distribution of elements.

b) Disadvantages of Laser cladding

1. Rough surface finish as compared to the parts produced by conventional methods[20]

2. Disturbances in the process can result in the poor clad properties[21].

3. High initial investments and lower efficiency of the laser source are one of the main limitations of laser-based manufacturing techniques [22].

4. Right from the raw material to processing, creating a suitable environmental condition is very important.[22]

5. The metal powders used in Additive Manufacturing are microscopic in size which are toxic, combustible and reactive in nature.

6. As laser is high energy beam source, the working person must be aware of its alignment.

2.7 CO₂ laser machine setup

2.7.1 Laser Gantry

The laser gantry is responsible for the movement of the Laser head over the build plate. So the precise movement of this laser gantry decides the accuracy of the profile which will be scanned and sintered during each layer. This in turn will decide the accuracy of the printed model. The laser head that is mounted on this gantry is supposed to move in an X-Y plane above the build plate.

Motion is obtained from stepper motors. Rotary motion is transferred from motor to linear motion with the help of Timing belt-pulley assembly; thus, giving motion to the laser head. Laser beam projects perpendicular to the X-Y plane. For one rotation of the motor, linear movement is: 20*2 = 40 mm (Pulley teeth" pitch of the teeth). When it Comes to accuracy in motion and power transmission, belt drives are more accurate than gear drives.

Once the movement of the Laser Gantry was functional, the next step was to align the Laser Reflecting mirrors along the Laser Gantry to direct the Laser ray from the source toward the Laser head and then to the Build plate The mirrors have to be aligned at precise angles as the

ray coming from the previous angle should be received at the center of the receiving mirror. These mirrors are aligned using adjustment screws that control the mirror's orientation. Once the alignment is completed the laser can be fired and the Laser gantry is fully functional.

Fig.2.12 Laser Gantry

The lens used in the Laser head has a focal length of 50 mm. Due to this condition, extender was needed to be manufactured for adjusting the distance between the lens and the build plate.

2.7.2 Enclosed inert gas chamber (Build Chamber)

A lens is a transmissive optical device that focuses or disperses a light beam by means of refraction[22]. A simple lens consists of a single piece of transparent material, while a compound lens consists of several simple lenses (elements), usually arranged along a common axis. Lenses are made from materials such as glass or plastic and are ground and polished to the desired shape. A lens can focus light to form an image, unlike a prism, which refracts light without focusing. Devices that similarly focus or disperse waves and radiation other than visible light are also called lenses, such as microwave lenses, electron lenses, acoustic lenses, or explosive lenses.

The main purpose of the enclosed chamber is to control the environment inside the chamber and create desired sintering conditions during the operation. The closed chamber needs to have provisions for the circulation of inert gas, which will be crucial in avoiding the oxidation of metal powder while sintering. With the inert gas circulation, a heating unit also has to be installed in the chamber to sense and control the temperature inside the chamber. The enclosed chamber was made using Mild-Steel Sheets. An inlet and an outlet for the inert gas circulation were provided in the chamber. The remaining gaps were finally sealed using

neutral silicone sealant, an acrylic glass was installed on the top plate of the chamber for a view of the operation while running.

An optical lens is mainly used for focusing in order to obtain higher-order power density. But it was found that the reflectivity of the lens and the plasma generated due to higher temperature damaged the lens. As a result, lens breaks. Also, this single lens costs around Rs.6000 to get replaced with the new one. So avoiding lens breakage is of prime importance.

Argon gas which was earlier provided at the bottom of the bed need to be additionally provided just below the nozzle head to break the contact between formed plasma and lens. For which argon gas must be supplied with higher flowrate. So that a square slit assembly having just 1mm of opening was made and installed just below the nozzle head. This provision has insured that the lens will not break even at the higher temperature.

2.7.3 Electronic Components

The electronic components are responsible for the control system of the machine which will be integrated with the mechanical components and used to control the movements of the mechanical components using the stepper motors used.

The Electronic setup mainly consists of following major components which will control the SLS system, they are:

- Stepper motors
- Micro-step Stepper drivers
- MACH3 (5-axis breakout Interface board)
- MACH3 software
- CO₂ Laser

2.7.4 Software programming

Software is necessary to control the electronic components of the machine as well as to carry out operations on the developed machine using G-codes and M-codes. To run an SLS, its axes are to be controlled. Another way of controlling SLS axes is by using CNC operating tools; which control five or six-axis Special Purpose Machines (SPM). Treating our SLS as an SPM, the software which has been used here, called Mach3 comes into the picture. Mach3 software is used to control all the operations on the developed unit.

A 3D model is to be created in any of the modeling software. The created 3D model is then sliced using slicing software which in this case will be CURA. Once the model is sliced, the created G-code program is obtained from this software and is modified a bit according to the

requirements of the SLS metal printer. This modified G-code program is then loaded on the Mach3 interface and is used for running the operation.

2.8 Effect of process parameters on processed samples

2.8.1 Effect of power and scanning speed on bonding

A study on laser cladding a stainless steel plate with a copper-based powder has been done by using a 100W blue direct diode laser system [23]. It was fabricated with three different powers (56 W, 74W and 96W) and seven scanning speeds starting from 1mm/s to 7mm/s. Surface properties and bonding between the base metal and powder were investigated. At a scanning speed of greater than 5 mm/s with a laser power of 56 W film formation was not achieved. When the scanning speed increases, the input energy to the substrate decreases. In the laser cladding process, substrates are required to be heated to achieve better metallurgical bonding between the substrate and powder material. when the scanning speed was greater than 5 mm/s the input energy was not enough to heat the substrate which resulted in no film formation.

On the other hand, at the slowest scanning speed, poor adhesions were obtained except at the laser power of 74 W. This result shows that too slow scanning speed tends to result in obtaining poor adhesion of film formation. Moreover, under several conditions, a number of porosities were seen inside films as shown in Fig.2.13It is reported that the number of porosities tends to increase when the laser power is relatively low to the powder mass flow rate. Therefore, the results in Fig.2.13 indicate that the laser power of 93 W is not enough for the powder mass flow rate of 17 mg/s to melt powder sufficiently.

2.8.2 Effect of cladding thickness on porosities

A study was done on SS316L steel In-vessel components of fusion reactors by cladding copper layer to improve the vertical stability of the plasma [24]. This plasma vertical instabilization is a serious concern as it causes the melting of In-vessel components. So in this work, a copper powder having powder particle size <63 µm and >63 µm was used for cladding a layer of 1mm and 3mm thickness.

Top surface radiography analysis was done to investigate the pores distributed in the claddings. Both the claddings with 1mm and 3mm layer thickness showed the presence of finely distributed pores. The pore size for the 1 mm-thick cladding was found to be smaller as compared to the 3 mm-thick cladding, which could be due to the difference in particle size of

the feedstock powders. From cross-sectional views, it was observed that the 1mm-thick cladding has shown (Fig.2.14a) lesser porosity or defects in comparison to 3 mm-thick claddings.
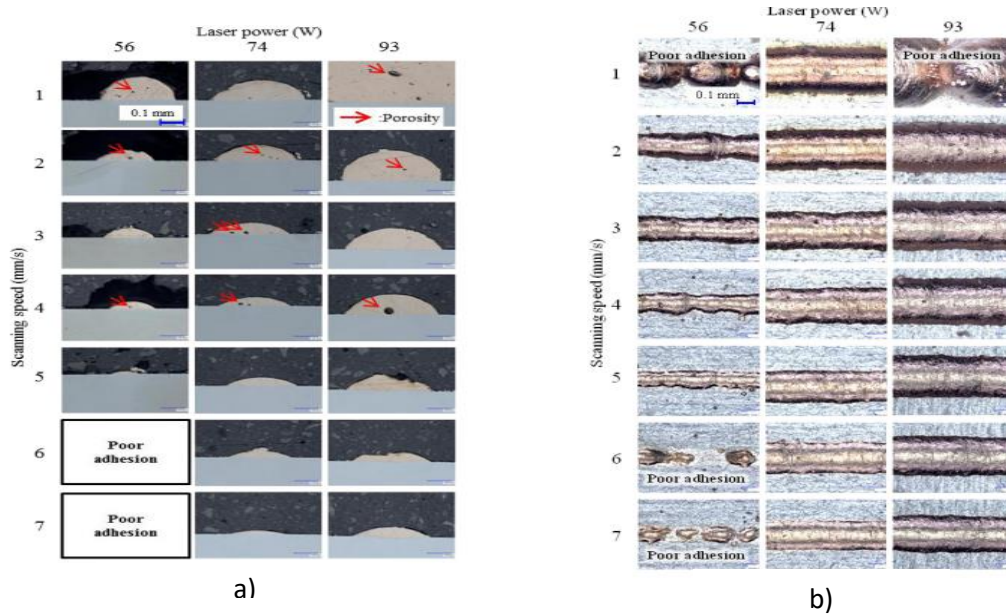

a)

b)

Fig.2.13 a) Surface images of copper film. b) Cross-section images of a copper film[23].

Pores of 0.2 mm to 0.6 mm in size were observed in near-edge regions of the 1mm-thick cladding, which are attributable to improper melting or heating of the samples owing to delay in melt pool formation or over travel speed of the nozzle. However, the 3 mm-thick cladding showed the presence of distributed porosity and inclusions at some places (Fig.2.14b) which may be due to relatively larger particle size of feedstock powder and voids resulting from evolution of gases [24].

2.8.3 Effect of beam diameter on clad geometry outputs

A study for better process optimization of SS316L substrate has been done using a laser cladding process in which substrate was cladded with pure copper powder by a CO_2 laser. It was found that as the laser beam diameter increases the temperature and stress profile decreases .Because as the beam diameter increases the more surface area gets heated but at a constant input power. This will increase more mass addition and melting pool but lesser will be the heat input because power will be distributed over the surface [21].
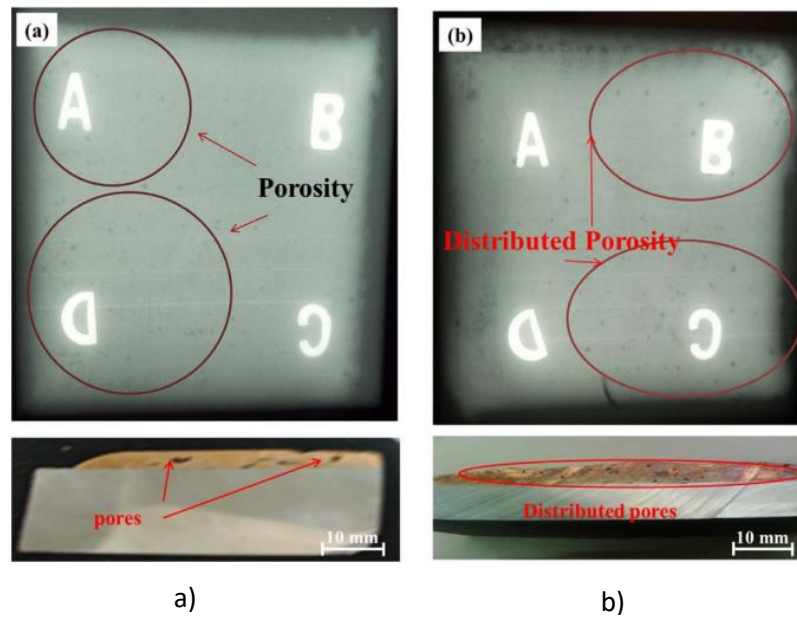
Fig.2.14 Surface and cross-sectional radiography analysis of laser claddings on SS316 steel showing the presence of pores (a) 1 mm-thickness (b) 3 mm-thickness[24].
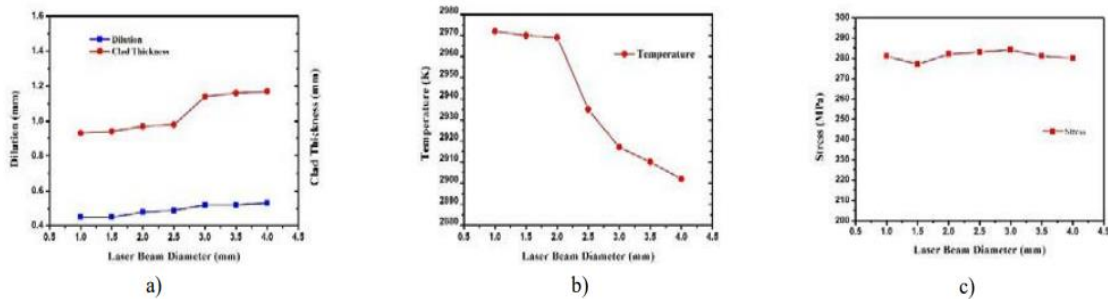
Fig.2.15 (a) laser beam diameter effects on dilution & clad height; (b) effects on temperature;(c) effects on stress [21].

2.8.4 Balling phenomena

Balling phenomena is the most common phenomenon associated with laser sintering [22]. In laser sintering, balling phenomena may result in a formation of discontinuous scan track and it leads to non-uniform deposition of fresh powder on the previous sintered layer. So the laser sintered sample shows the tightly packing of balls.

In this work, two types of balling phenomena during laser sintering were investigated and the metallurgical mechanism of balling was explained. In the first type of balling phenomena, the
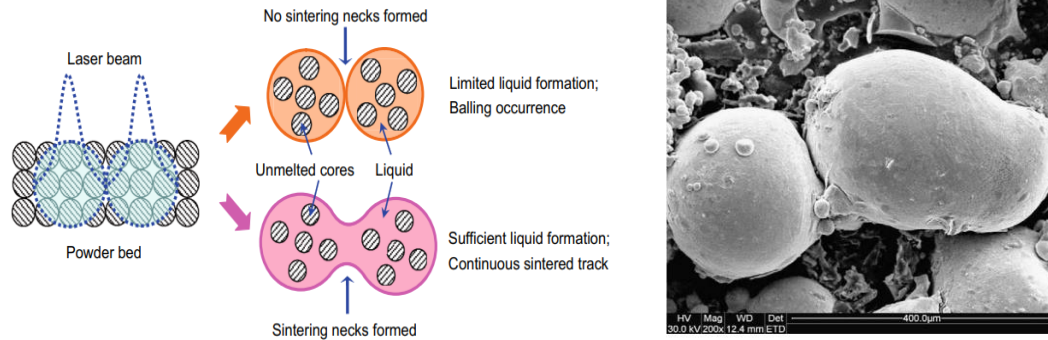
Fig.2.16 Schematic and SEM image of balling phenomenon caused by limited liquid formation [22].

amount of liquid formation depends upon the sintering temperature and this temperature depends on two main parameters i.e. laser power and scan speed during single laser line scanning. For a given scan speed, super-solidus sintering temperature decreases with lowering the laser power, resulting in a smaller amount of liquid formation. Thus the viscosity of the liquid-solid mixture becomes considerably high slowing down the liquid flow and particle arrangement. This in turn decreases the overall rheological performance of the liquid in conjunction with solid particle. Consequently, the molten material in each spot irradiating zone tend to aggregate into an individual coarsened sphere approximately the diameter of laser beam as shown in Fig.2.16. The liquid formation affect the bonding between the balls formed as shown in the Fig.2.17.
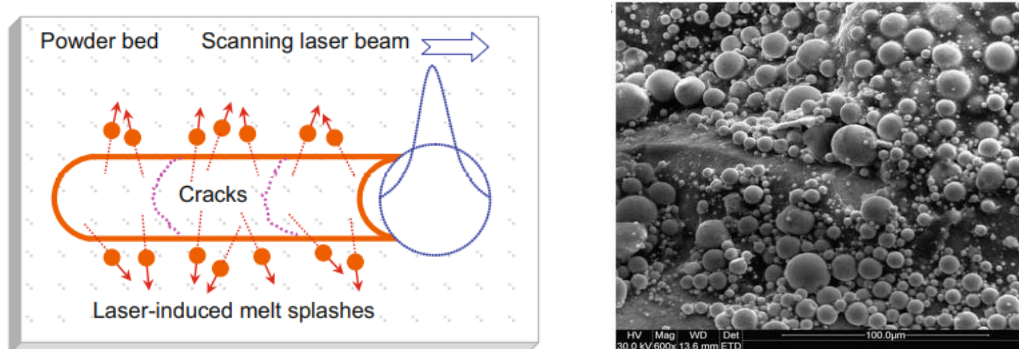
Fig.2.17 Schematic and SEM image of the second kind of balling phenomenon characterized by small-sized balls on the sintered surface .caused by melt splashes during laser scanning [22].

In the micro-scaled of balling phenomena shown in Fig.2.17b, micrometer-scaled balls are formed by melt splashes. When a sufficient amount of liquid phase is generated by using a relatively high laser power (400 W), laser sintering at high scan speed tends to shape the melt into a continuous cylindrical molten track, due to a considerably short dwelling time of laser

spot on each irradiating region. However, the present molten track is in a highly unstable state. The surface energy of the liquid track will keep decreasing, in order to obtain a final equilibrium state. With increasing the scan speed used, the linear energy density of laser input decreases, resulting in a decrease in the working temperature and, accordingly, the diameter of the cylindrical molten track. The melt instability, consequently, increases significantly. Under this condition, a number of small-sized liquid droplets tend to splash from the surface of the molten track, due to the reduction in the surface energy of liquid at short length scales. After solidification, a large amount of micrometer-scaled spherical splashes are formed around the sintered surface, resulting in the micro-scaled balling phenomenon as shown in Fig.2.17b [22].

It is noted that at an even higher scan speed (10 m/s in this study), a significantly elevated instability of the liquid cylinder tends to alter its shape to reduce the surface energy, besides the occurrence of the micro-scaled balling effect. This causes the breaking up of the molten cylinder to reach a final equilibrium state, thereby producing longitudinal cracks in the finally solidified tracks.

2.9 Summary

The literature survey shows that the laser cladding process is a complex but quick process of 3D printing with metallurgical and chemical phenomena. It mainly depends on many laser parameters consisting of laser power, beam diameter, mode of laser, pulsed frequency pulse width, layer thickness, particle size distribution are important. Laser cladding setup requires XYZ laser head manipulation system, powder spreading mechanism and controlled atmosphere using chiller and argon gas.

1. The most important defect observed in the laser cladding is balling phenomenon. This balling phenomenon is mostly attributed to the laser power density. The proper combination of laser power and scanning speed must be maintained to achieve the required power density.

2. Sintering in an argon atmosphere is preferred over a nitrogen atmosphere because porosity increases due to the absorption of nitrogen during the sintering process.

3. The laser position parameters which includes beam diameter, hatch space and scanning strategy plays in important role in deciding density and porosity of the final samples.

4. It is important to select the appropriate laser sintering parameters to perform successful laser sintering process. It was found that there are number of parameter, which affects

properties of sintered part Laser parameters, process parameters and material characteristics are summarized in the cause effect diagram as shown in fig.
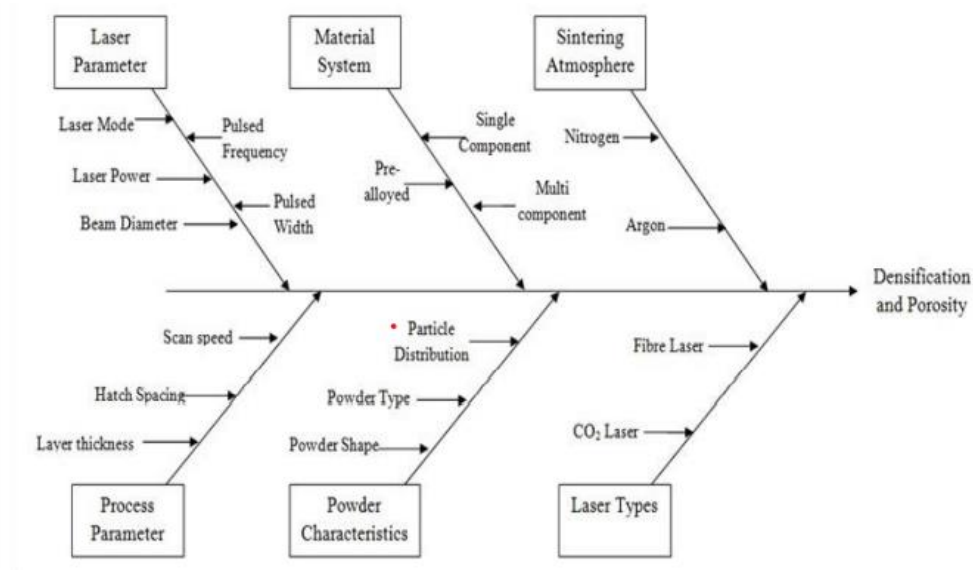
Fig.2.18 Cause and effect diagram of Laser Sintering[4].

2.10 Objectives

From the discussion of literature survey ,in this work, laser cladding of copper powder on mild steel substrate is performed with variation in parameters like laser power (power density), scan speed, hatch spacing, direction of scanning and number of layers. Effect of these parameters was studied on hardness, bond shear strength, density, porosity and microstructure. The copper powder was characterized for particle-size, apparent density and flow and following objectives were decided.

1. To develop the pre-build selective laser sintering (SLS) machine to perform laser cladding.

2. To perform laser cladding of pure copper powder by varying laser power and scanning speed.

3. To study the effect of laser scan direction on density, porosity and secondary dendrite arm spacing by conducting the microstructural analysis.

To optimize bond shear strength and micro-hardness of copper cladded specimen.

CHAPTER 3

EXPERIMENTAL WORK

To attain the objective of this project work, need to modify the CO$_2$ laser machine available in the college. The machine consists of a laser head that can move in X and Y directions whereas the bed can move in Z direction. It also consists of a powder spreader/ roller to lay the powder along the bed. The modifications were done in creating an inert atmosphere so that the problem of lens breakage gets eliminated. It was followed by laser cladding experiments where it needs to find the effect of varying the laser parameters and laser position on the bond shear strength, density, porosity and secondary dendritic arm spacing of the clad material. It was decided to perform the experimental work as shown in fig.3.1

3.1 CO$_2$ laser machine setup

For this experimental work CO$_2$ laser machine having a maximum power of 200 W with a laser beam diameter of 0.6 mm was used. An experimental setup consists of a CO$_2$ laser machine, a moving laser head and a chiller. The flow diagram for the laser cladding experiment is shown in Fig.3.4 The specification of the laser machine, CNC XY-table and Mega Chiller are shown in Table.3.1
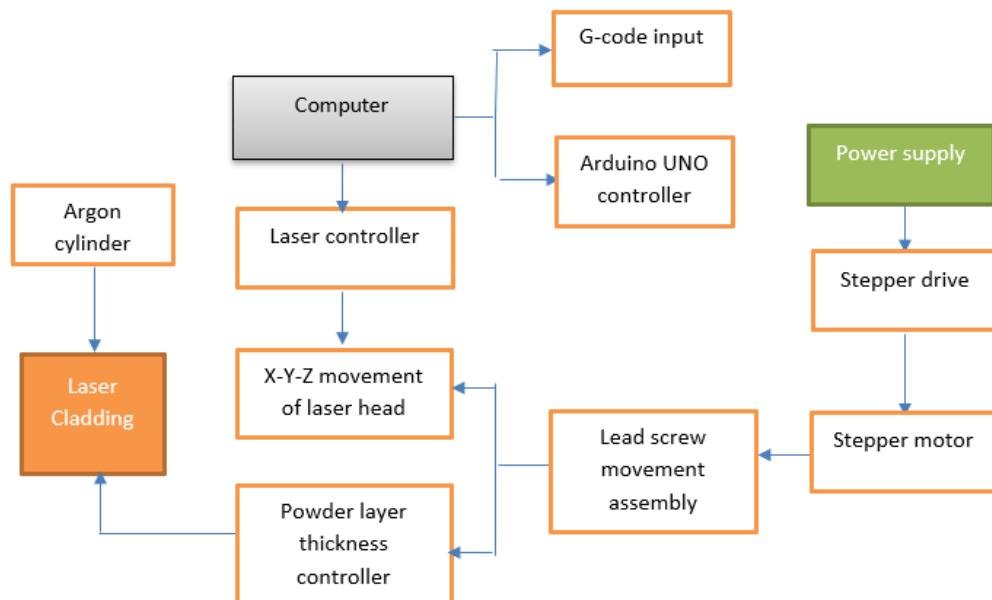
Fig. 3.1. Schematic diagram of the working process of laser cladding.

A mega chiller is used to remove the heat produced in the laser machine during the laser generation. A water cooling mixture was used to remove the heat generated in the laser head, in which cold water was entered from one end and hot water is out from other end of the laser head jacket .

3.1.1 Fixing the argon gas setup

A lens is a transmissive optical device that focuses or disperses a light beam by means of refraction. A simple lens consists of a single piece of transparent material, while a compound lens consists of several simple lenses (elements), usually arranged along a common axis. Lenses are made from materials such as glass or plastic and are ground and polished to the desired shape. A lens can focus light to form an image, unlike a prism, which refracts light without focusing. Devices that similarly focus or disperse waves and radiation other than visible light are also called lenses, such as microwave lenses, electron lenses, acoustic lenses, or explosive lenses.

An optical lens is mainly used for focusing in order to obtain higher-order power density. But it was found that the reflectivity of the lens and the plasma generated due to high temperature damaged the lens. As a result, lens breaks as shown in fig. Also, this single lens costs around Rs.6000 to get replaced with the new one. So avoiding lens breakage is of prime importance. A newly installed lens after a week of working is shown in fig.3.2

a)   b)

Fig. 3.2 a) lens before installing b) Lens after 1 week of experimentation.

Argon gas which was earlier provided at the bottom of the bed needs to be additionally provided just below the nozzle head to break the contact between the formed plasma and lens. Argon gas must be supplied with a higher flow rate. So a square slit assembly having just 1mm of the opening was made and installed just below the nozzle head. This provision has insured that the lens will not break even at the higher temperature.
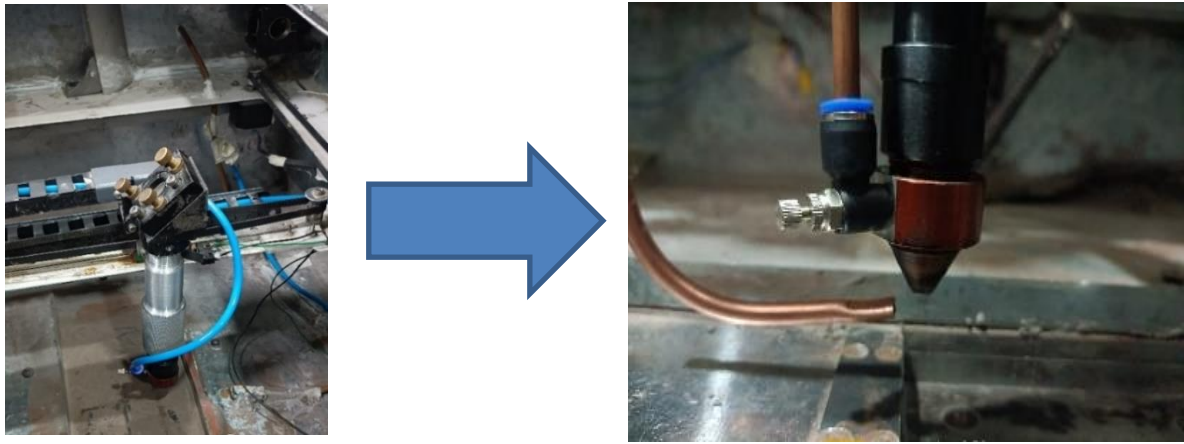
Fig. 3.3 Changes made in the CO2 laser machine to avoid lens breakage
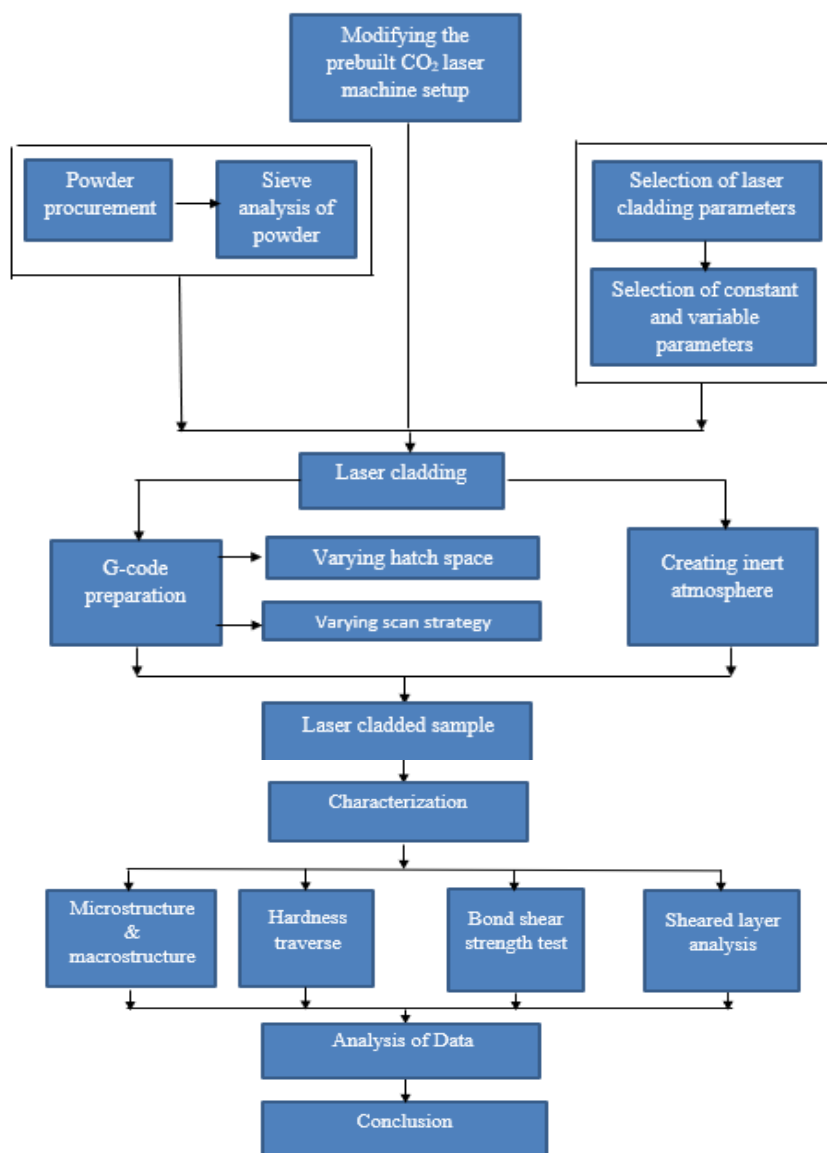
Fig.3.4. Flowchart of experimental work for laser cladding.

3.1.2 Machine specifications

Table 3. 1 Machine Specifications

CO$_2$ laser Specifications	
Laser Type	Gas laser
Max. Output Power	200 W
Beam Excitation	RF
RF Power Supply	Integrated
Wavelength	10.6 μm;
Beam Characteristics	K > 0.8
Pulse Frequency (PP)	0 - 130 kHz
Speed limits	100 mm/s
XYZ Laser head manipulation system specifications	
Stroke Length in X, Y and Z direction	1350 × 1350 × 100
No. of Start of X', Y and Z axis lead screw	1
Pitch of X & Y axis lead screw	6 mm
Pitch of Z-axis lead screw	4 mm
Controller	Arduino Uno & GRBL
Speed limits in X and Y direction	0.1 mm/s- 80 mm/s
Speed limits in Z direction	0.1 mm/s- 50 mm/s
X, Y axis stepper motor	NEMA34-128 Kg.cm
Z-axis stepper motor	NEMA23-22 Kg.cm
Power supply for X',Y axis stepper motors	6 Amp, 60 VDC
Power supply for Z-axis stepper motor	4.2 Amp, 24-48 VDC
Load carrying capacity	100 Kg
Mega chiller	
Sensor Type	NTC Thermistors
Resolution	0.5 ⁰C
Accuracy	±1 ⁰C
Controlling Temperature Range	30⁰C to + 50⁰C

3.1.3 Design of Mechanical setup

a. Stepper motor was coupled with lead screw and ball bearings. The movement of the frame depends on the rpm of lead screw, pitch and lead.

b. Lead screw was designed with a single start by considering the required speed.

c. As per the design, the dimensions of a lead screw are 30 mm in diameter and 1450 mm in length. Mild steel (EN8) material was selected for the lead screw and followed by blackodising, because of self-lubrication and it prevents corrosion.

d. Y and Z-axis frames were considered as X-axis as shown in Fig.3.5 and Fig.3.6. Therefore during the X-axis movement, Y and Z-axis frames are moved.

e. To observe translational displacement in the Z direction, analysis of the Y-axis frame is necessary.
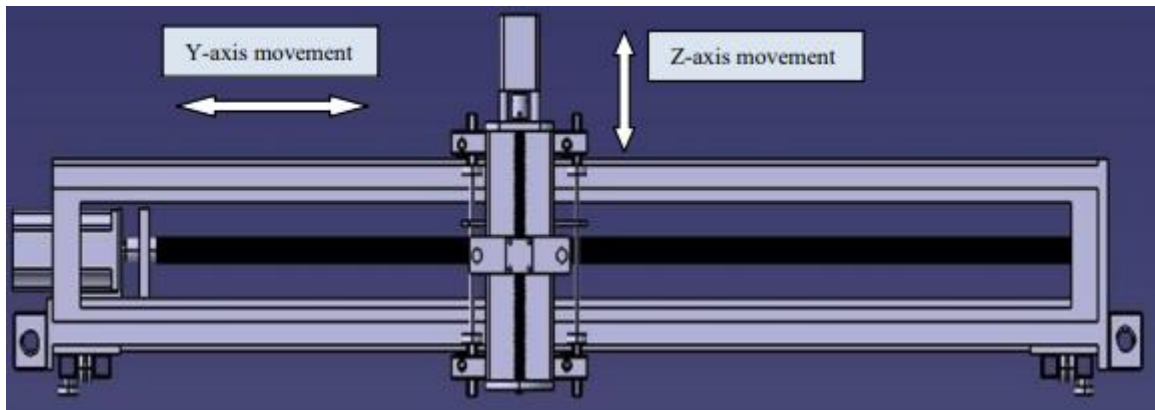
Fig.3.5 Y and Z axis movement of the laser head.
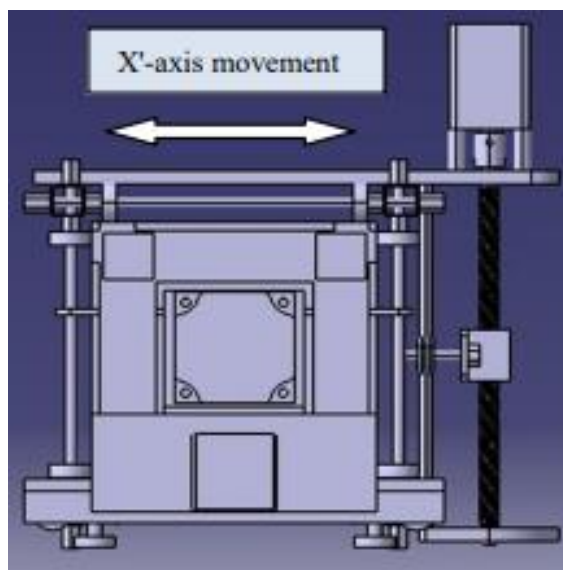
Fig.3.6. Side view of Y and Z-axis frame shows X'-axis movement

a)   b)
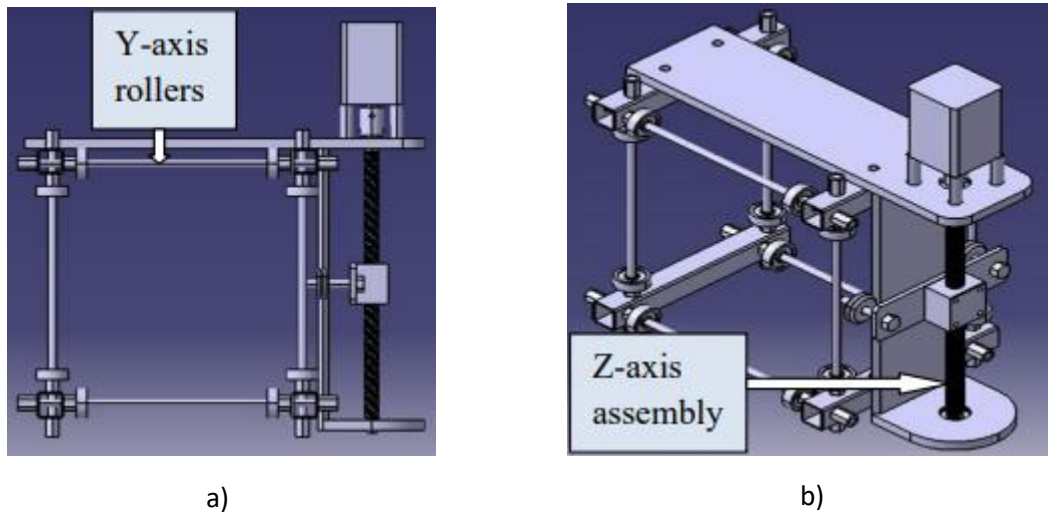
Fig.3.7 a) Y -axis rollers and Z-axis assembly b) Y-axis rollers and Z-axis assembly
3D view

3.2 Powder Procurement and characterization

For this experimental work, the pure copper powder was selected. It has different particle sizes and shapes and distributions. After procuring copper powder, particle shape and size were observed under the Scanning electron Microscope. Characterization was done by calculating the apparent density flowrate of the powder, size and shape distribution. The powder was also pre-heated to remove the moisture content in the powder as powder was unable to flow during the first experimentation.

3.2.1 Sieve Analysis

A sieve analysis is a procedure used to access the particle size distribution of a granular material by allowing the material to pass through a series of sieves of progressively smaller mesh size and weighing the amount of material that is stopped by each sieve as a fraction of the whole mass.

The size distribution is often of critical importance to the way the material performs in use. A sieve analysis can be performed on any type of non-organic or organic granular materials including sands, crushed rock, clays, granite, feldspars, coal, soil a wide range of manufactured powders, grains and seeds, down to a minimum size depending on the exact method.

Sieve analysis of pure copper powder was done on the sieve analyser machine available in the college to check the particle size distribution. For experimentation 100 gm of powder used and screened using the sieves of 25 μm, 37 μm, 45 μm, and 53 μm.
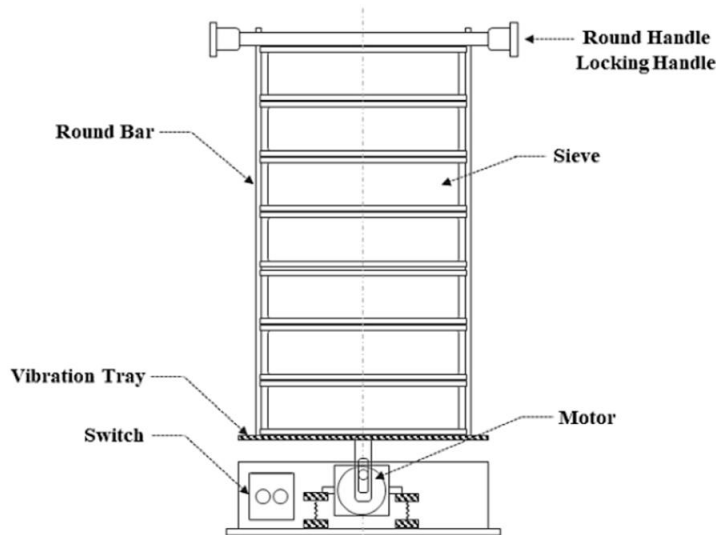
Fig.3.8. Schematic of sieve analyser.

3.2.2 Apparent Density

Apparent density is also called bulk density, packing density and bed density in the Powder bed manufacturing process [25]. The flow ability of a metal powder affects its behavior in Additive Manufacturing (AM) production. Moisture content, morphology, and particle size distribution are the parameters that can influence flow. The apparent density of both powders was measured with the help of the Hall flowmeter as shown in figure 3.9.

According to the B212 standards, the flowmeter determines the apparent density by permitting a certain quantity of powder in a loose condition to flow from a hall flowmeter funnel orifice diameter of 0.1 inches into a specified cup of a definite volume ($25cm^3$). The discharge powder from the orifice at the bottom of the funnel is blocked with a dry finger, and the powder is poured into the funnel without any tapping, vibration, or movement of the funnel. The mass of powder per unit volume is recorded as apparent density. This experiment was repeated 10 times to get the average value of apparent density.

$$Apparent\ Density = \frac{Final\ wt - Initial\ wt}{Volume\ of\ the\ cup} \quad \ldots \ldots \ldots \ldots \ldots \ldots Eq.(3.1)$$

Apparent density is directly proportional to the particle size, decreasing the particle size decreases apparent density, because the smaller the particle size greater will be the surface area of the powder which subsequently increases the friction between the particles and decreases the apparent density. Particle shape also affects the apparent density, particles with a less spherical shape causes increased frictional surface area and less uniformity in powder packing which results in decreased apparent density.

33

3.2.3 Flow-rate

Many industrial application like die filling, powder transfer, and powder spreading depends upon the flowability of the powder. It is the time required for the powder sample of a standard weight to flow under the atmospheric conditions through the funnel of the hall flow meter, a lower flow rate indicates better flowability.
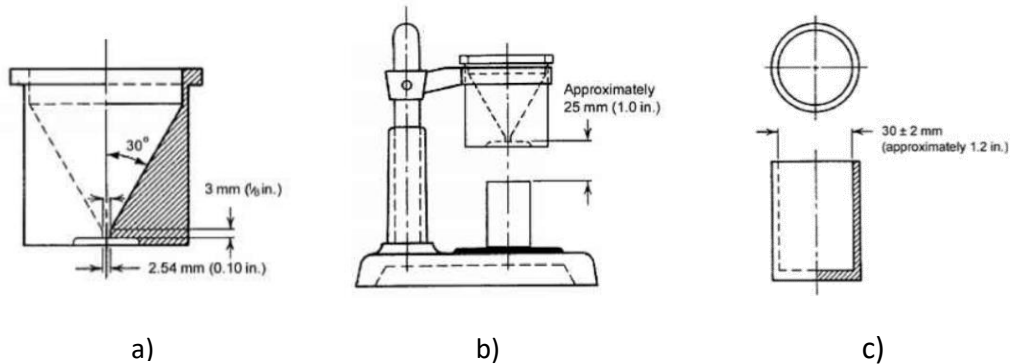
Fig.3.9. a) Hall funnel b) Equipment Assembly c) Density cup [25].

According to the ASTM B213 standard, to perform the test, 50 grams of both powders were selected and allowed to flow through the hall funnel of fixed geometry. The hall funnel used has an opening of 2.5 mm, a cone angle of 60° and ten times repetitions were performed as powder characteristics are influenced by the frictional, gravitational, and atmospherical conditions.

3.2.4 Scanning Electron microscopy (SEM) analysis

Scanning electron microscopy (SEM) is a microscopic technique used for analysis at higher magnification and with a higher depth of field. Higher magnification allows much detailed investigation of different phases which are non-detectable on an optical microscope can be detected using SEM. SEM is carried out on FE-SEM (Field Emission-SEM) by ZEISS. EDS work on the principle of X-ray microanalysis, when electrons are bombarded on the specimen electrons are knocked out from the specimen this will allow electron from the upper shell to go to the lower shell, which will form an x-ray with characteristic wavelength and energy. This energy can be detected and used for spectroscopy. SEM analysis was done to check the morphology of a bought pure copper powder. By using this chemical composition, morphology of the powder and sintered sample can be predicted.

3.3 Laser cladding Experiments

Laser cladding was done on a pure copper powder having powder size between (30-40µm) with different parameters like power density, speed, hatch distance and scan strategy.

Focusing lens having a focal length of 63.5 mm was used to reduce the laser beam diameter from 4mm to 0.6mm. Experiments were carried out by cladding square samples (20mm ×20 mm) and with different layers. The argon gas flow, laser beam diameter and laser mode were kept constant.

Table 3.2 Design of experiment for square samples with beam diameter 0.6mm.

Sr.No	Laser Power(W)	Scan Speed (mm/s)	No of layers	Hatch Space (mm)	Scan strategy
1	80	8	1	0.5	H
2	80	8	2	0.5	H
3	80	8	3	0.5	H
4	80	8	4	0.5	H
5	100	8	1	0.5	H
6	100	8	2	0.5	H
7	100	8	3	0.5	H
8	100	8	4	0.5	H
9	140	8	1	0.5	H
10	140	8	2	0.5	H
11	140	8	3	0.5	H
12®	140	8	4	0.5	H
13	140	10	3	0.5	H
14	140	13	3	0.5	H
15	140	10	3	0.25	H
16	140	10	3	0.5	H
17	140	10	3	0.6	H
18	170	10	3	0.5	H
19	170	10	3	0.5	V
20	170	10	3	0.5	D

Square samples were prepared for the experimental purpose to check hardness, surface morphology, sintered sample density and microstructure. It was decided to make samples of 20mm × 20mm and varying thicknesses. For laser cladding 0.6 mm diameter was used, therefore the hatch space was kept below 0.6 mm for continuous cladding. Overlapping of 0%,17% and 60% were made to reduce porosity between two adjacent tracks. For 0%

overlapping distance between two successive tracks was kept 0.6mm, for 17% overlapping it was 0.5 mm and for 60% overlapping it was 0.25mm. Different scanning strategies like horizontal, vertical and diagonal were also used to study the effect on porosity and shear strength of cladded samples.

a)   b)   c)
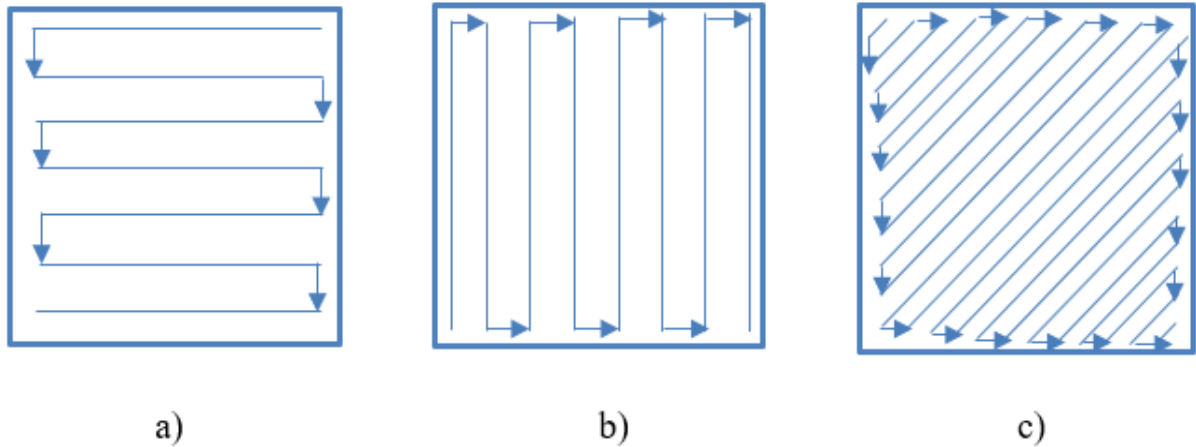
Fig. 3.10. a) Horizontal b) Vertical c) Diagonal scan strategies

Table 3.3 Process parameters used for laser claddings

Sr.No.	Laser Parameters	Value
1	Laser Mode	Pulsed
2	Beam Diameter	0.6 mm
3	Laser Power	80W,100W, 140W
	Process Parameters	**Value**
4	% overlapping	0%,17%,60%
5	Scan strategy	Horizontal, vertical, diagonal
6	Scan speed	8 mm/s, 10 mm/s, 13 mm/s
	Material Parameters	**Value**
7	Powder	Pure copper
8	Powder Size	35 µm
9	Powder shape	Spherical
	Other Parameters	**Value**
10	Argon Gas Flow	Continuous.
11	Room Temperature	25^0 C

3.3.1 Calculations for surface temperature

During selective laser sintering irradiation is given by Eq.(2.2)

For laser beam diameter of 0.6 mm, surface temperature is calculated.

Parameters assumed for pure copper powder,

- Thermal conductivity, K= 50 W/Mk.

- Thermal Diffusivity, $\alpha = 1.38 \times 10^{-5} \, m^2/s$.

Table 3.4 Change in power density and surface temperature with change in power and scan speed.

Power (W)	Beam diameter (mm)	Power density (W/mm2)	Scan speed (mm/s)	Interaction time (sec)	Surface temperature (°C)
80	0.6	283.085	8	0.075	2124.925
80	0.6	283.085	10	0.06	1871.769
80	0.6	283.085	13	0.0461	1608.087
100	0.6	353.857	8	0.075	2724.406
100	0.6	353.857	10	0.06	2407.961
100	0.6	353.857	13	0.0461	2078.359
140	0.6	495.399	8	0.075	3923.368
140	0.6	495.399	10	0.06	3480.346
140	0.6	495.399	13	0.0461	3018.902

The surface temperature was calculated by using Eq.(2.2) and the graph of surface temperature vs power density is shown in fig.3.11
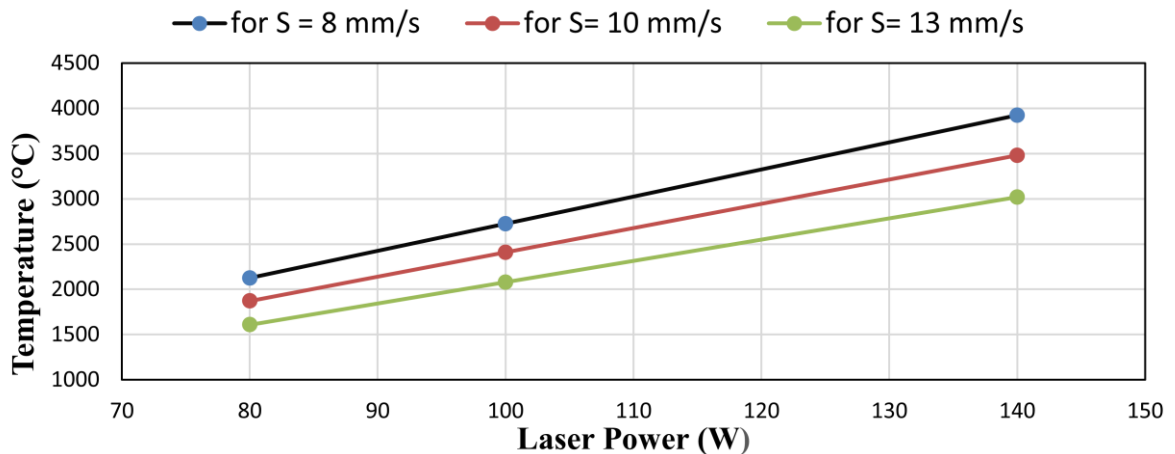
Fig. 3.11. Effect of laser power on surface temperature by varying the scan speed

microstructural images of sample. While selecting the microstructural images, images with 100x magnification were selected.

The density measured by Archimedes' principle has some errors due to the penetration of water into the pores.

$$Actual\ density = \frac{Wt\ in\ air}{Wt\ in\ air - Wt\ in\ water} \times density\ of\ water \quad ......$$

$$...............\ Eq.(3.2)$$

$$Relative\ density = \frac{Actual\ density}{Theoretical\ density} \times 100 \quad ....\ Eq.(3.3)$$

The percentage porosity of sintered sample was measured from the relative density by using the equation

$$Porosity\ \% = 100 - Relative\ porosity ....\ Eq.(3.3)$$

3.3.2 Hardness testing

Hardness was measured by a microhardness testing machine on an HV scale. An indentation is made on the specimen by a diamond indenter through the application of 100 gf load and dwell time of 10 seconds. The size of the indent formed on the surface was measured using the calibrated optical microscope.

3.3.3 Microstructure

The square samples were observed under an optical microscope at 100X , 200X, 500X , 1000X and 2000X magnifications. Observations were done to analyse the change in microstructure from substrate to the outermost cladded layer. Samples with different laser power, scanning speed, hatch space and scanning strategy were prepared for the microstructural study. The etchant used was100 ml of ethanol +25 ml of HCL +5 gm of FeCl$_3$ and the etching time was about 5 seconds. Images were taken on the image analyser to find the secondary dendritic arm spacing (SDAS) at 500X

3.3.4 Bond shear strength test

Bond shear strength was conducted on the universal testing machine (UTM) available in the college. External fixture for clamping the sample during test was required so that sample does not deflect during the test. The load vs distance plot for all the samples were plotted in the software from which maximum load obtained.
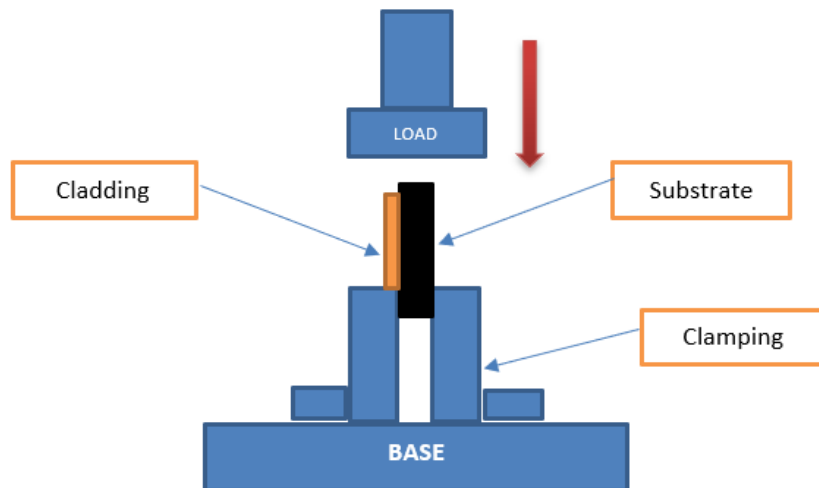
Fig.3.12. Bond shear strength test setup.

CHAPTER 4
RESULT AND DISCUSSION

4.1 Laser cladding setup

The CO_2 laser machine available in the college required maintenance like laser beam alignment, cleaning the reflecting mirrors, installing the lens and renewing the coolant before starting the experimentation. The laser cladding setup is shown in fig. 3.1, argon was used to prevent oxidation. Argon is inert gas hence it does not take part in the reaction also it has a higher density than other gases, therefore, it forms a layer above the powder which was to be cladded and oxidation was prevented during laser sintering.

4.2 Apparent Density and Flowrate

The apparent density and flow rate of as received pure copper powder was measured with the help of a Hall flowmeter by using Eq.(3.1) and it was found to be 2.9 g/cc and 35 sec/50gm respectively.

Initial wt. of density cup before the powder was poured = 22.2568 gm.

Final wt. of density cup after the powder was poured = 94.7543 gm.

Apparent density = 2.9 g/cc

4.3 Particle size distribution of powder

A sieve analysis of copper powder was done to check the particle size and distribution. Instead of whole powder, a sieve analysis of 100g powder was done. As received copper powder was screened using sieves of 25 µm,37 µm,45 µm, 53 µm. Particle size distribution was also done by using the SEM image, the histograms were plotted by measuring the size of 20 particles captured at 500X magnification, and ImageJ software was used to calibrate and measure the particle size present in the picture. The SEM shows that the particle shape of the powder is spherical and also has some small satellite particles which decreased the flow rate of powder.

4.4 Results of cladded samples

As shown in Table 4.1 to Table. 4.4 , it shows the appearance of cladded samples. These samples were made by varying the laser power like 80W, 100W, 140W ; scanning speed like 8mm/s, 10 mm/s, 13 mm/s; Hatch space like 0.25mm, 0.5mm, .6mm, scanning strategy like horizontal, vertical, diagonal, and number of layers like 1,2,3,4 layers. By varying one

parameter and keeping all the other parameters same, two sets of 30 samples were prepared out of which 21 samples were selected. One set of 21 samples was used for mechanical testing and the other was used for microstructural analysis.
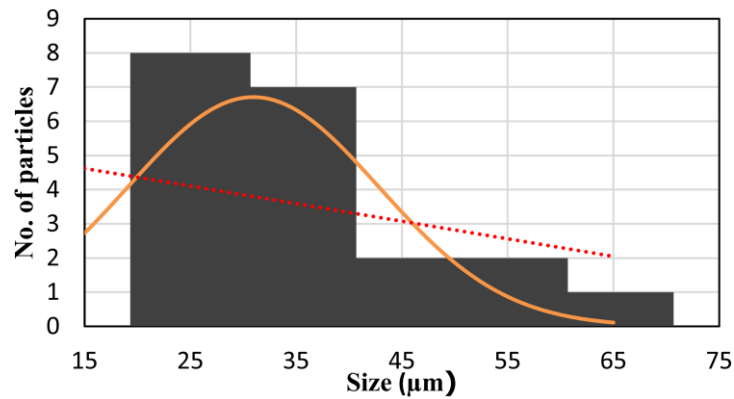
Fig. 4.1. Particle size distribution of pure copper powder.
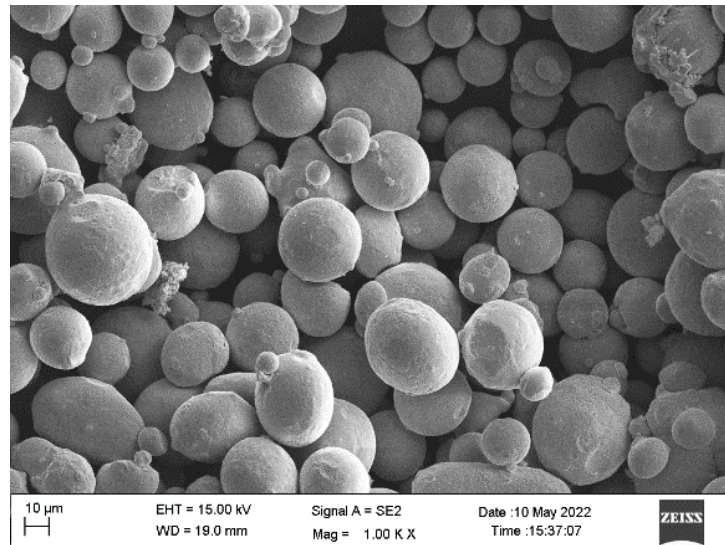
Fig.4.2. SEM image of copper powder at 1000x magnification

4.5 Density and Porosity

The density of sintered disc samples was measured from Archimedes' principle by using Eq.(3.10) and Eq.(3.11). The density of sintered sample depends on power density and interaction time . The calculated average density was found to be 3.41 g/cm^3 which is lesser than the theoretical density of copper. The difference in density of cladding is due to the presence of porosities in the sample.

The presence of porosity can be attributed to two reasons ie.

1. Improper melting or heating of the substrate and clad layer.

2. Delay in melt pool formation of a substrate.

Table 4.1 Appearance of laser cladded sample by varying number of layers and laser power.

Power \ Layers	1L	2L	3L	4L
80 W				
100 W				
140 W				

Table 4.2 Appearance of laser cladded sample by varying scanning speed and laser power

Power \ Scan Speed	8 mm/s	10mm/s	13 mm/s
140W			

Table 4.3 Appearance of laser cladded sample by varying hatch space and laser power

Hatch space / Power	0.25mm	0.5mm	0.6mm
140W			

Table 4.4 Appearance of laser cladded sample by varying scan direction and laser power

Scan Direction / Power	Horizontal	Vertical	Diagonal
170 W			

Porosity occurs due to oxidation of the powder or poor wetting between the substrate and the clad layer. The oxidized powder produces spherical pores. Improper wetting is found to be between the tracks where the interface angle is steep. The energy incident on the surface normal to incident beam is insufficient to re-melt both the previous track and the substrate. When the scanning speed increases, due to lower interaction time and improper melting, a melt pool will not form causing the porosity to increase from 12.96 %, 22.044%, 34.999% for scanning of 8mm/ sec, 10 mm/sec, 13 mm/sec respectively. For lower laser power also low melting will happen which results in poor adhesion and porosity. For the hatch space of 0.25 mm and 0.5 mm porosity was found to be 5.572% and 6.212 % respectively but for the hatch space of 0.6 mm porosity was 13.433 %. For the sample with 0.6mm hatch space there will be no overlapping which causes an increase in the porosity whereas for 0.25 mm and 0.5mm hatch space, there is overlapping of 0.35mm and 0.1mm respectively. Results showed the least porosity for the diagonal scanning strategy than the horizontal and vertical scanning strategies. The graphs of all the parameters with their porosity and density below.
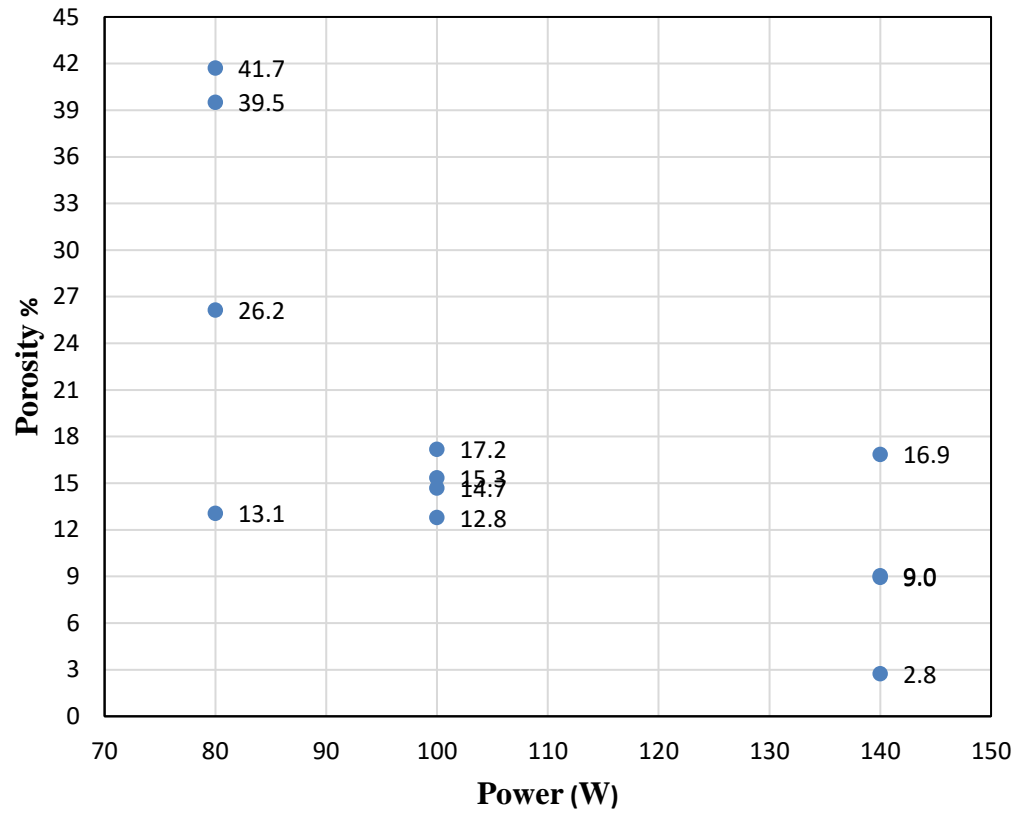
Fig.4.3 Effect of laser power on porosity %   of cladded specimen.
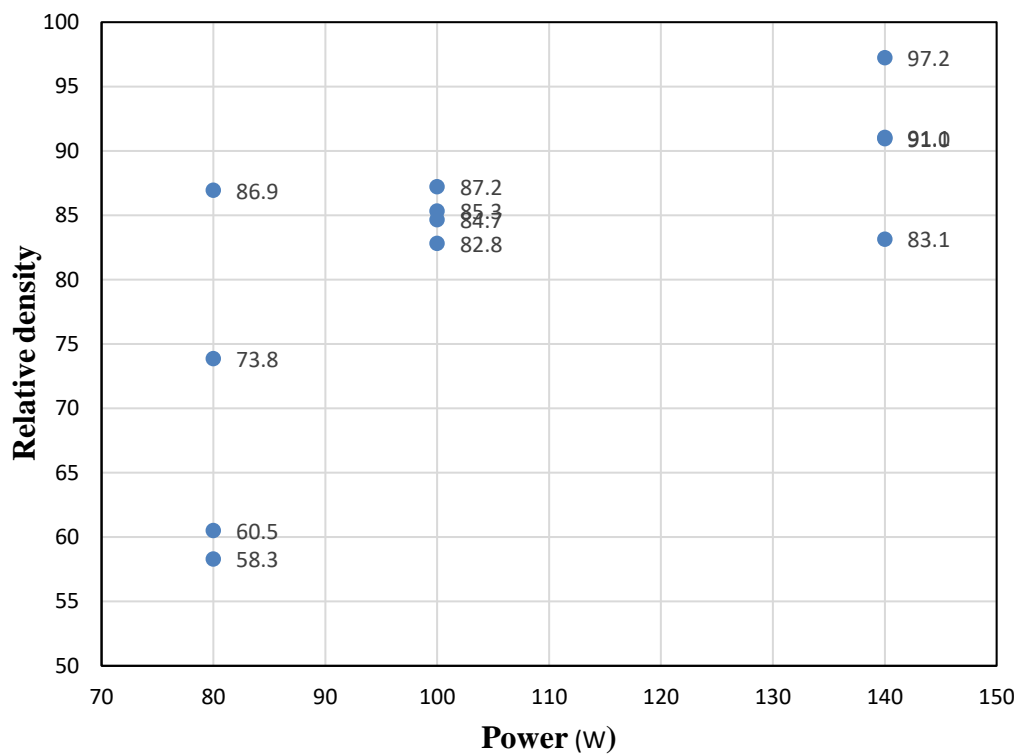
Fig.4.3 Effect of laser power on relative density of cladded specimen.
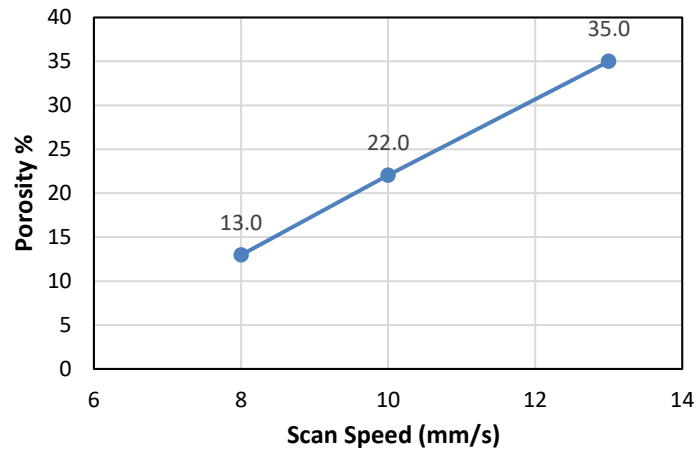
Fig.4.5 Effect of scan speed on porosity % of cladded specimen.
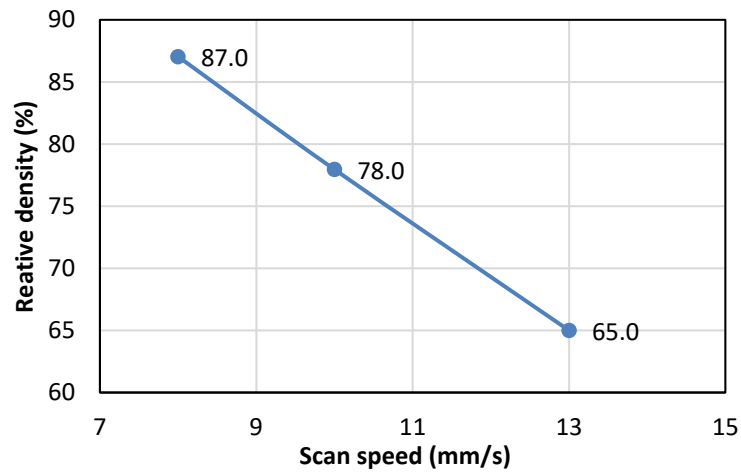
Fig.4.6 Effect of scan speed on relative density of cladded specimen.
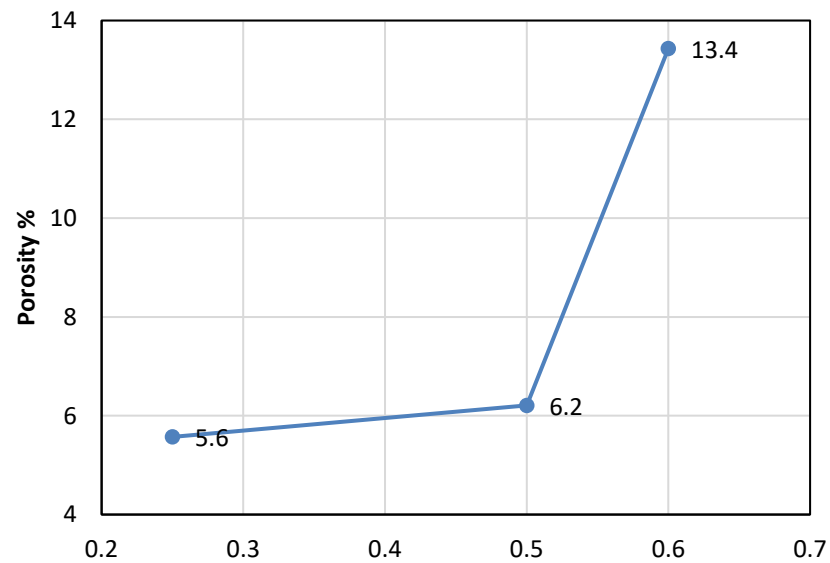
Fig.4.7 Effect of hatch space on porosity % of cladded specimen.
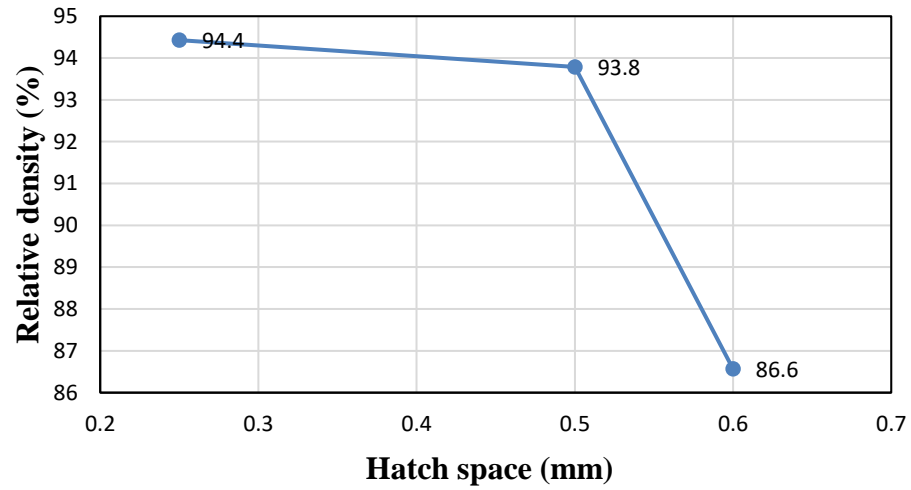
Fig.4.8 Effect of hatch space on relative density of cladded specimen.
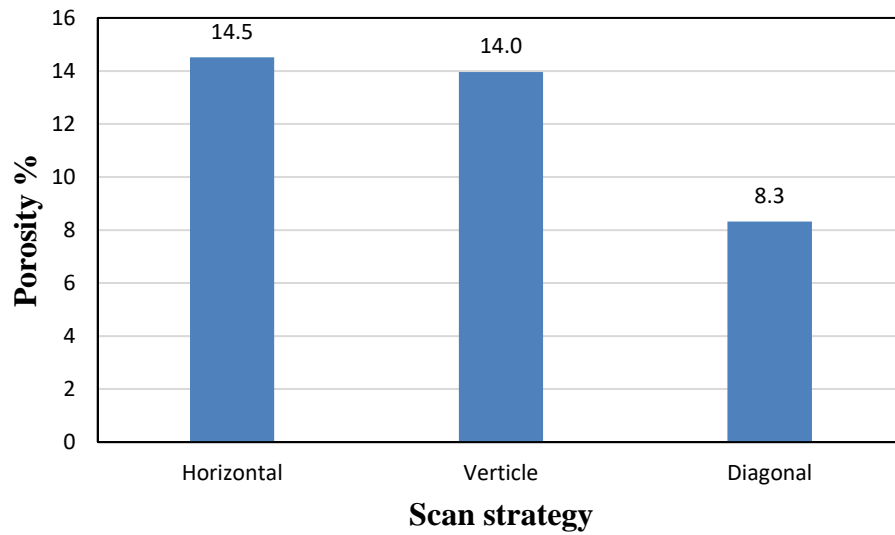
Fig.4.9 Effect of scan strategy on porosity % of cladded specimen.
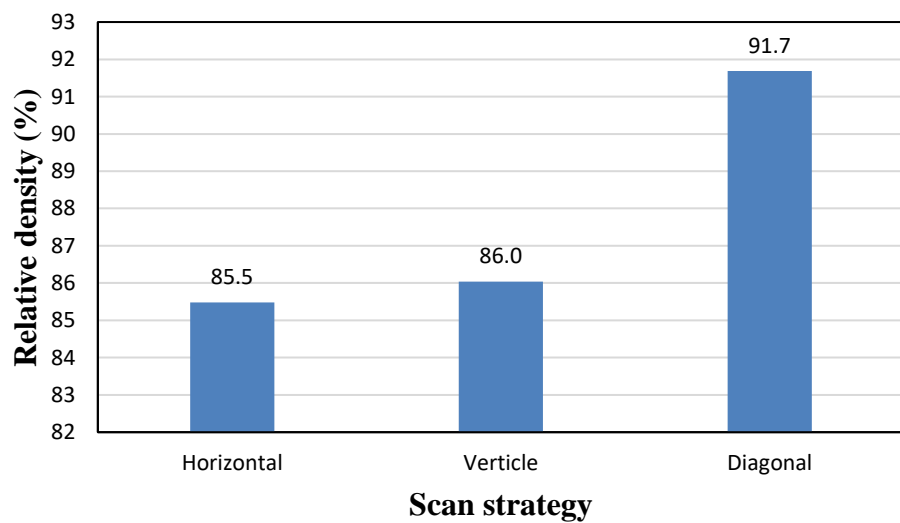
Fig.4.10 Effect of scan strategy on relative density of cladded specimen.

4.6 Microhardness

The microhardness measurements were carried out on the sample using the microhardness tester machine for which a load of 100gm and dwell period of 10 secs was used. The readings were recorded on steel substrate, the interaction of substrate and clad layer and on the pure copper claddings. For the substrate the average microhardness was found to be 125 HV, for the pure copper layer is in the range of 75 Hv – 105Hv.

4.6.1 Effect of power and number of layer variations on the microhardness

The highest microhardness was found to be near the substrate which can be attributed to the heat-affected zone (HAZ). The least microhardness was found at the interaction of the substrate and copper layer due to improper bonding. It was observed that as the number of layers increases the hardness goes on decreasing which can be occurred due to the increase in the size of grains. For the samples with 3 and 4 layers, the hardness showed a decreasing trend due to the grain growth of the previously deposited layer. The variation of microhardness with laser power for samples having 1- 4 layers was shown in fig.4.10 to Fig. 4.13.
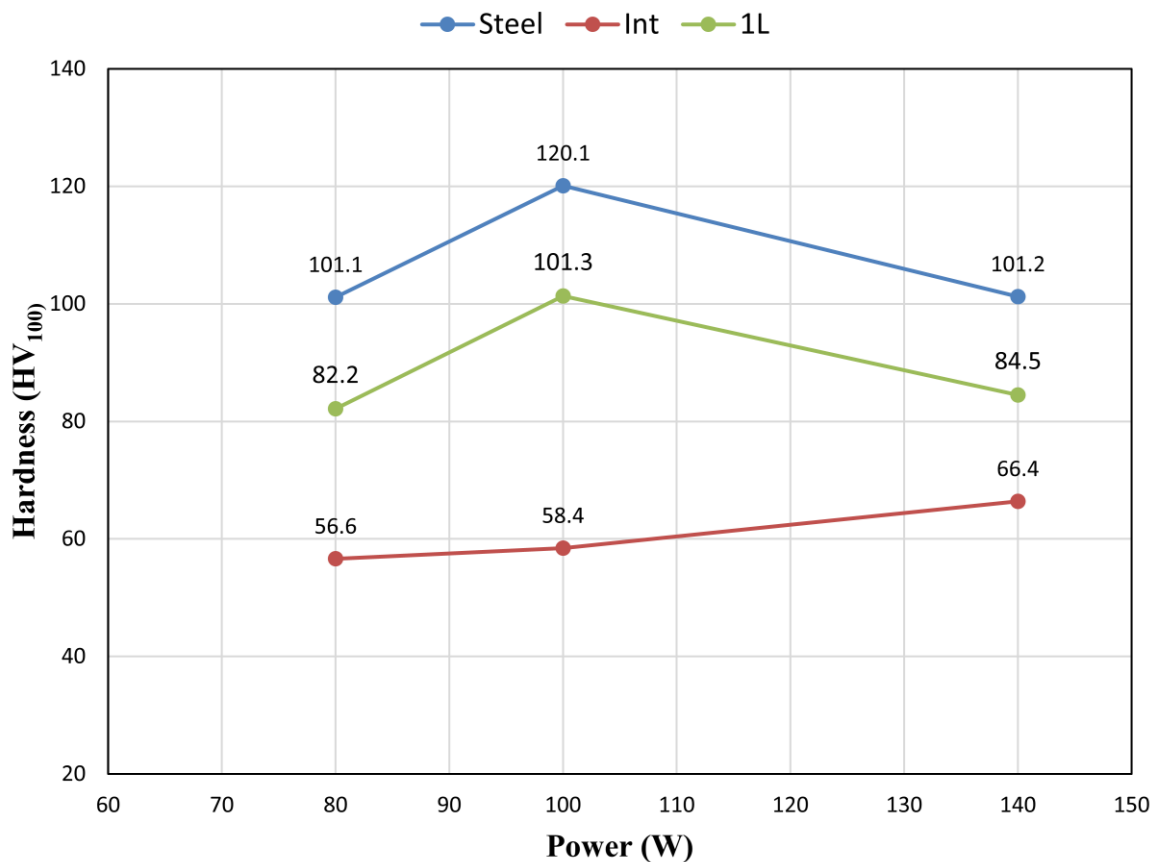
Fig.4.11 Effect of laser power on micro-hardness of specimen having 1 layer of copper.
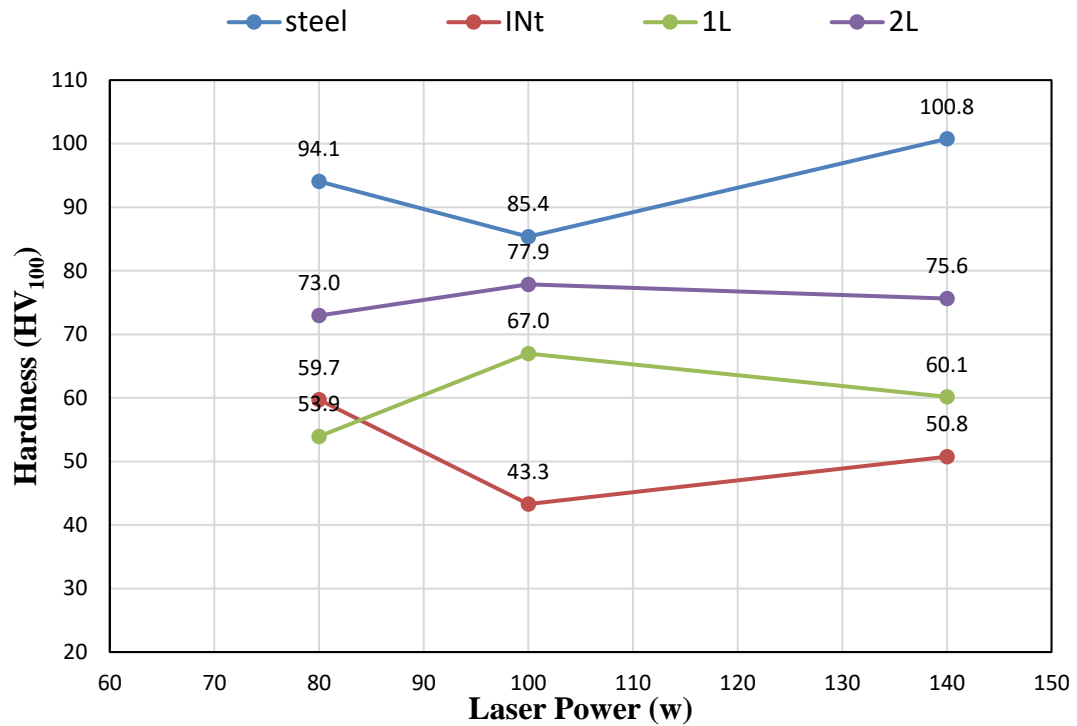
Fig.4.12 Effect of laser power on micro-hardness of specimen having 2 layer of copper cladding .
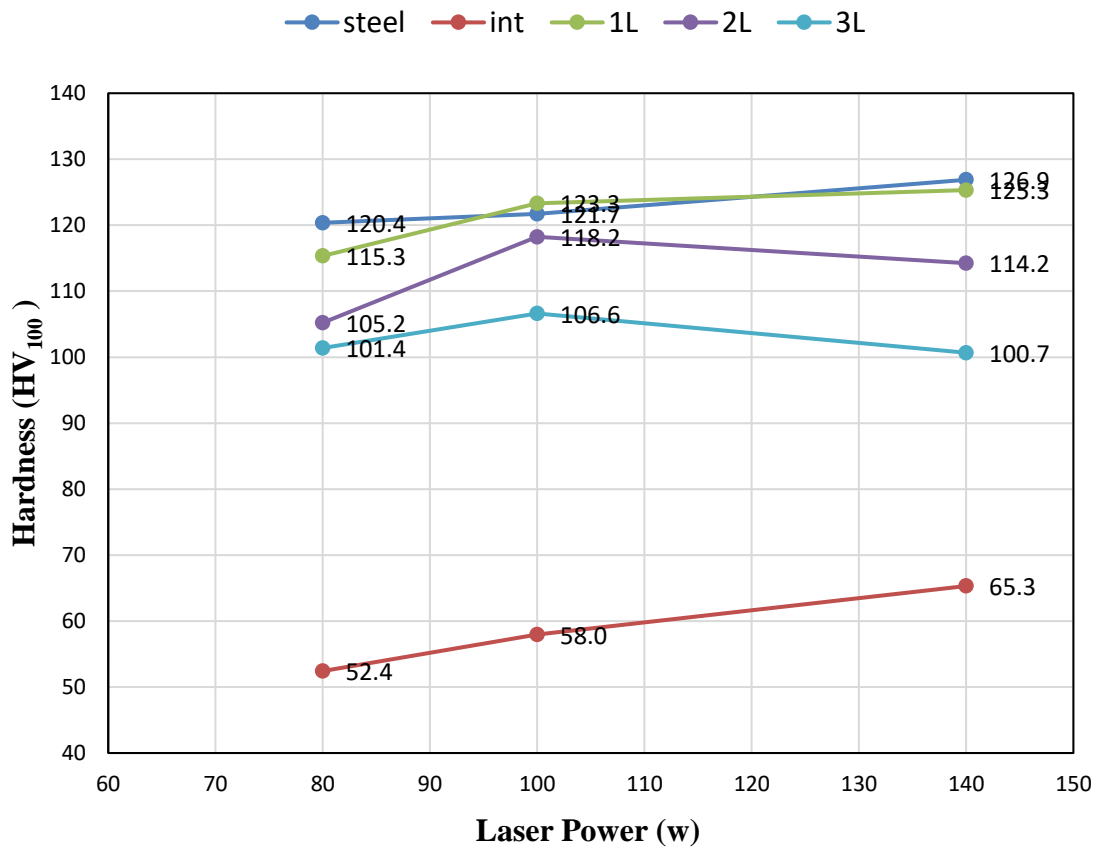
Fig.4.13 Effect of laser power on micro-hardness ofspecimen having 3 layer of copper cladding .
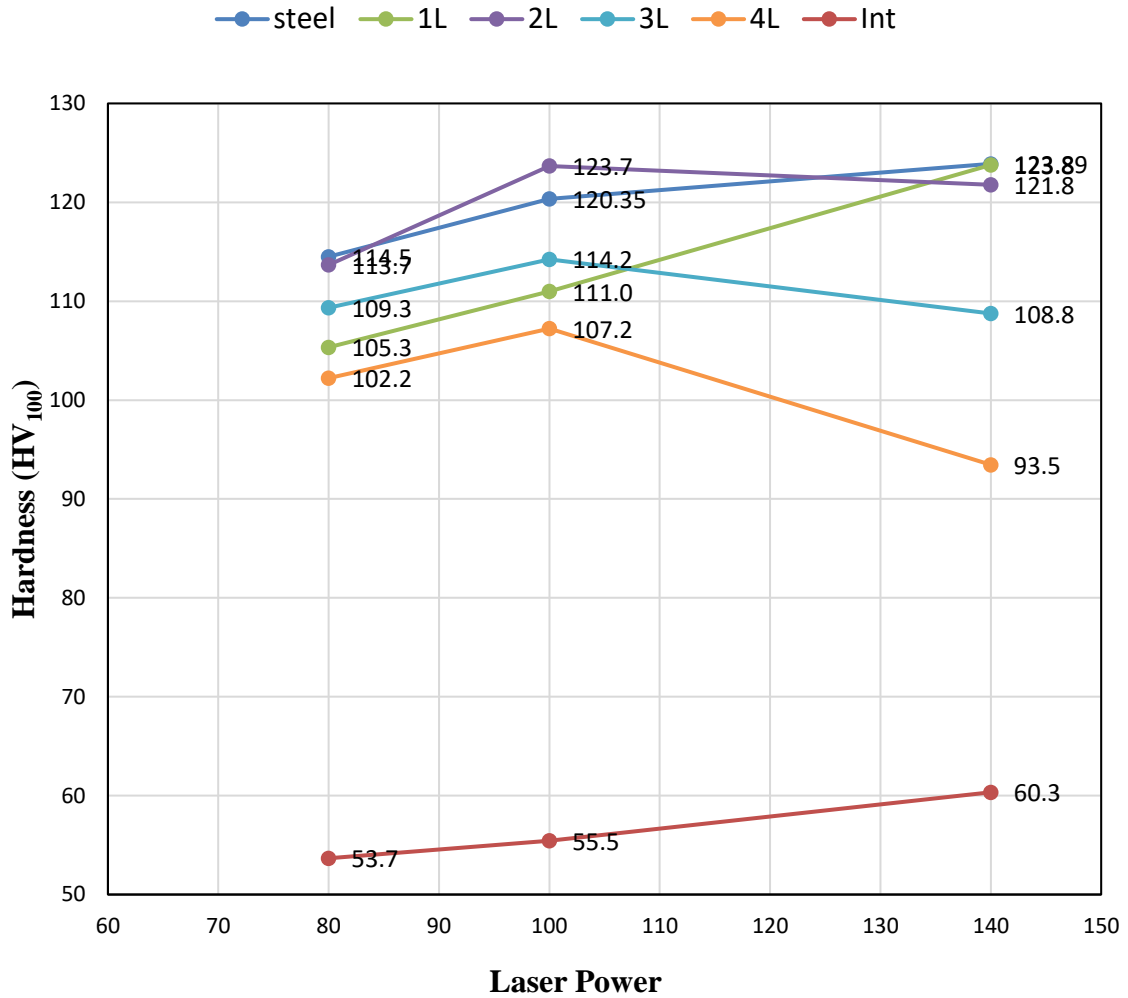
Fig.4.14 Effect of laser power on micro-hardness ofspecimen having 4 layer of copper cladding .

4.6.2   Effect of scanning speed on microhardness

Three samples were cladded with pure copper powder by varying scan speed and keeping the other parameters constant. For the experimentation three scanning speeds were selected ie. 8 mm/sec, 10 mm/sec and 13 mm/sec. Laser power of 140 W, hatch space of 0.5 mm and horizontal scanning strategy were used for cladding. The results of the change in the microhardness by changing the scan speed are plotted in fig Microhardness was observed to increase as the scan speed increased. Samples fabricated with a laser scanning speed of 8mm/ sec has the lowest hardness value, while sample fabricated with 13 mm/sec scanning speed has the highest hardness value. This increase in the hardness can be attributed to the grain refinement because as the scanning speed increases interaction time of the beam with the surface decreases avoiding grain growth.
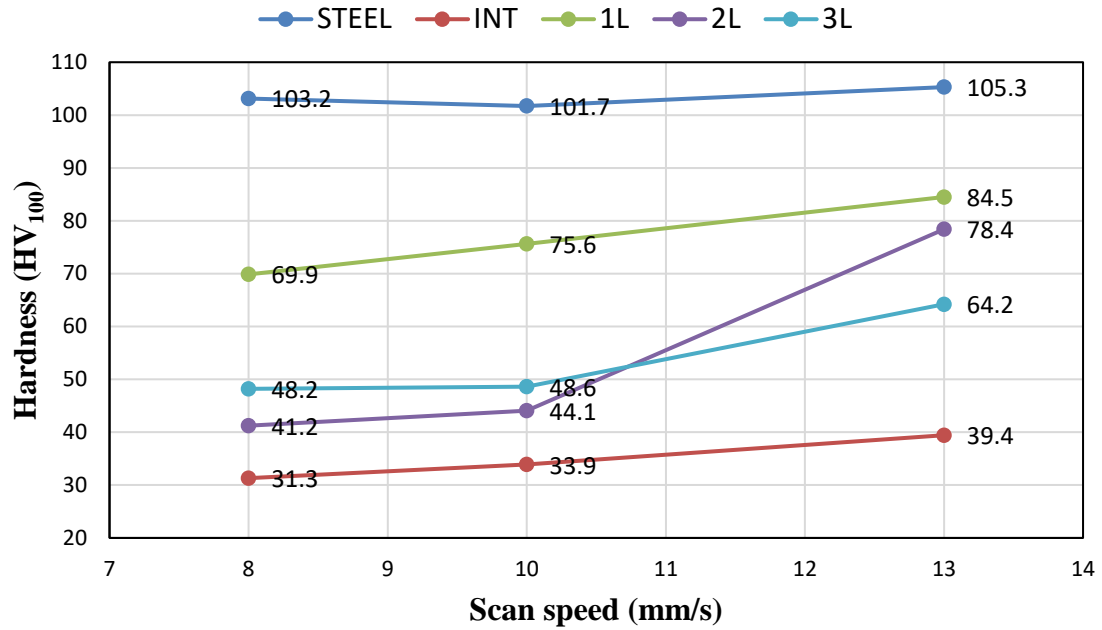
Fig.4.15 Effect of scan speed on micro-hardness ofspecimen having copper cladding .

4.6.3 Effect of hatch space on microhardness

Three samples with different hatch spaces like 0.25 mm, 0.5 mm and 0.6 mm by keeping other parameters constant like Power =140 w, speed= 10 mm/s, Scan strategy= H and Layers=3. With increasing the hatch space hardness showed a decreasing trend as the overlapping of the layer decreases as hatch space increases.
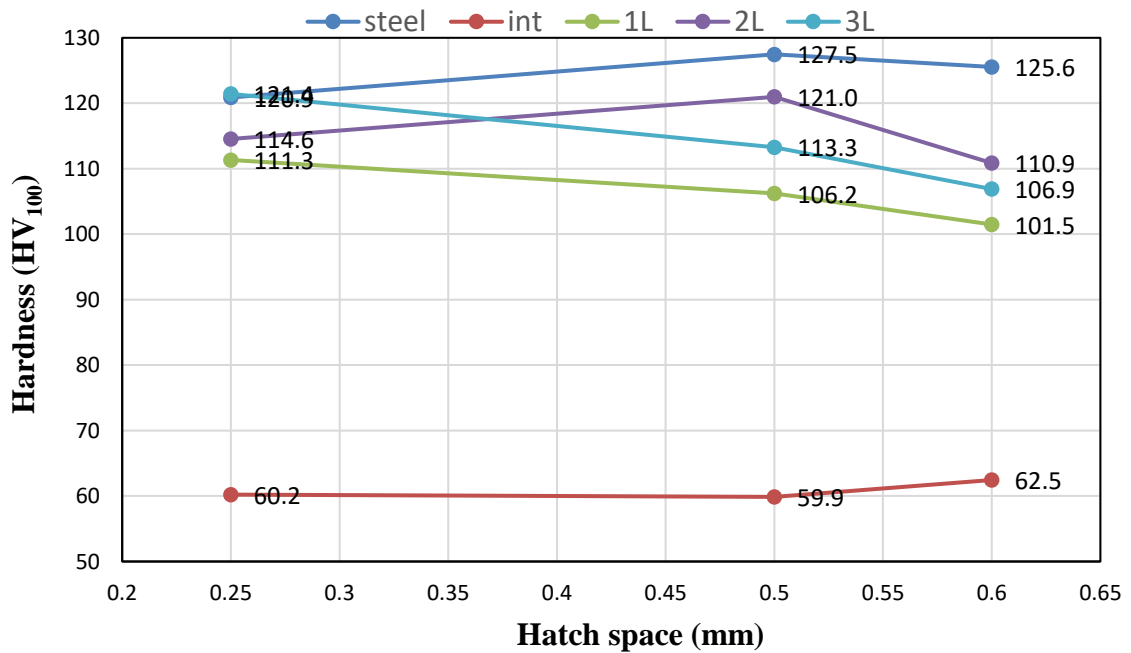
Fig.4.16 Effect of hatch space on micro-hardness ofspecimen having copper cladding .

4.6.4   Effect of scan strategy on microhardness

Three samples with three scan strategies like horizontal, vertical and diagonal were selected for cladding. Other parameters like Power=170 w, speed= 10 mm/s, hatch space= 0.5 and Layers=3 were kept constant. From the results, it was found hardness for the horizontal scan strategy showed good results compared to vertical and diagonal scan strategies. SDAS results showed a lower value for the horizontal scan strategy. So it can be concluded that the horizontal scan strategy has faster cooling rates which resulted in finer grains and good microhardness.
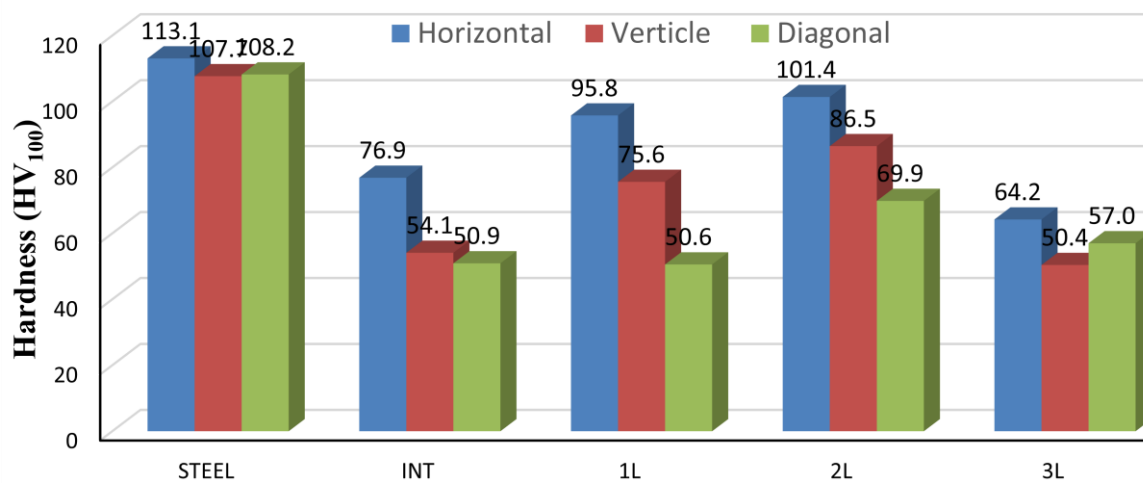
Fig.4.17 Effect of scan strategy   on micro-hardness ofspecimen having copper cladding .

4.7   Bond shear strength

The bond shear strength test was carried out on a Universal Testing Machine, for which extra clamping was required to hold the sample tightly during testing. For a three-layer sample fabricated with 80 W laser power, testing went wrong so the results of this sample are not mentioned in the figures below.

Fig.4.18 Bond shear strength test setup.
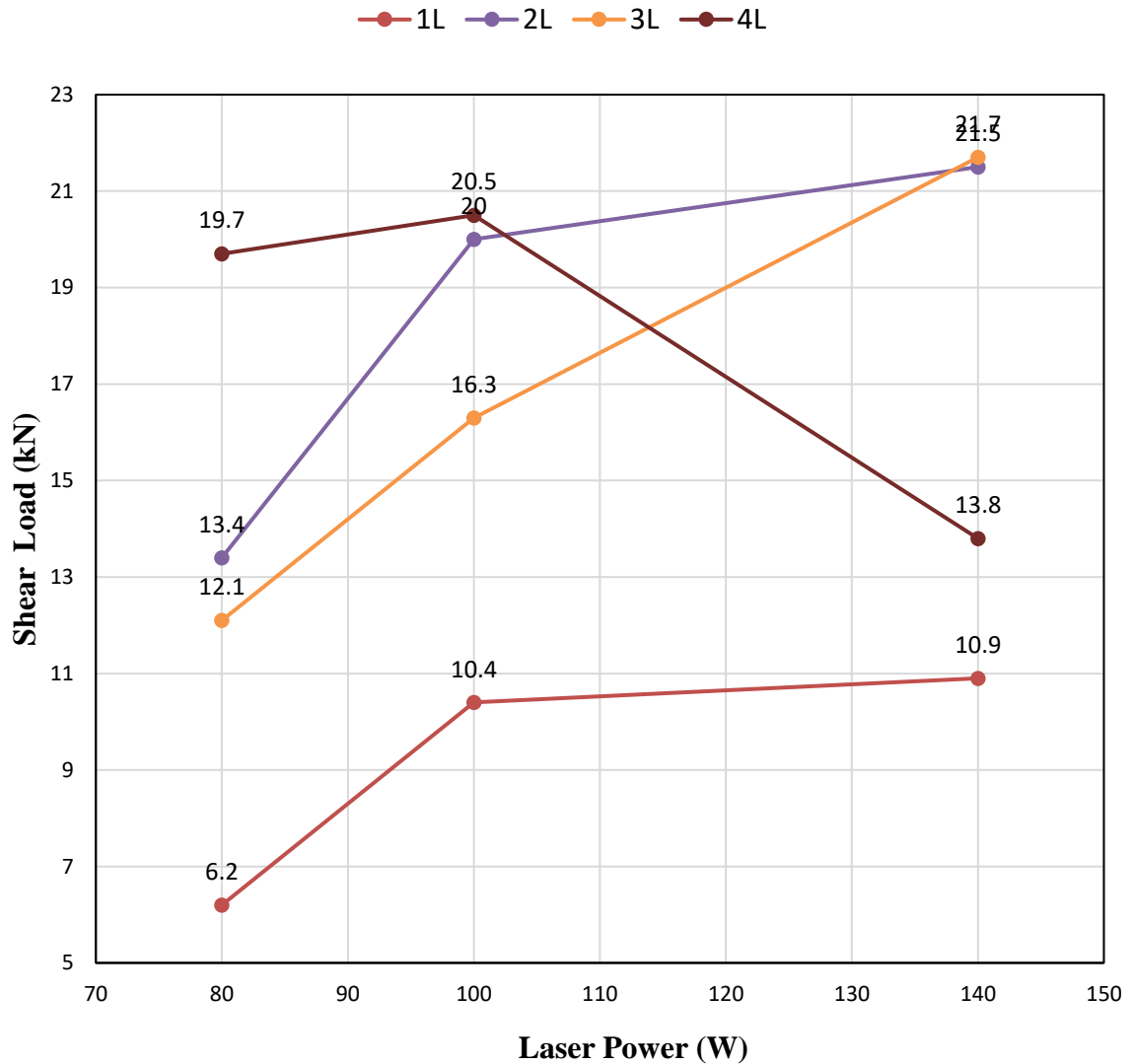
Fig.4.19 Effect of laser power on shear load of specimen having copper cladding of 1- 4 layers.

4.7.1 Effect of scan speed on bond shear strength

From the results mentioned in the fig below, it was observed that the maximum load taken before the shearing of the sample is 14.6 KN for the sample fabricated with 13 mm/sec scan speed, whereas for the sample produced with 8 mm/sec scan maximum load was 11.4 kN. For low scan speeds, cooling time and diffusion will be more , leading to an increase in the dendritic arm spacing. which also concludes the increased strength of the sample. For higher scan speeds, lesser interaction time and fine grain structure resulted in the higher shear strength.
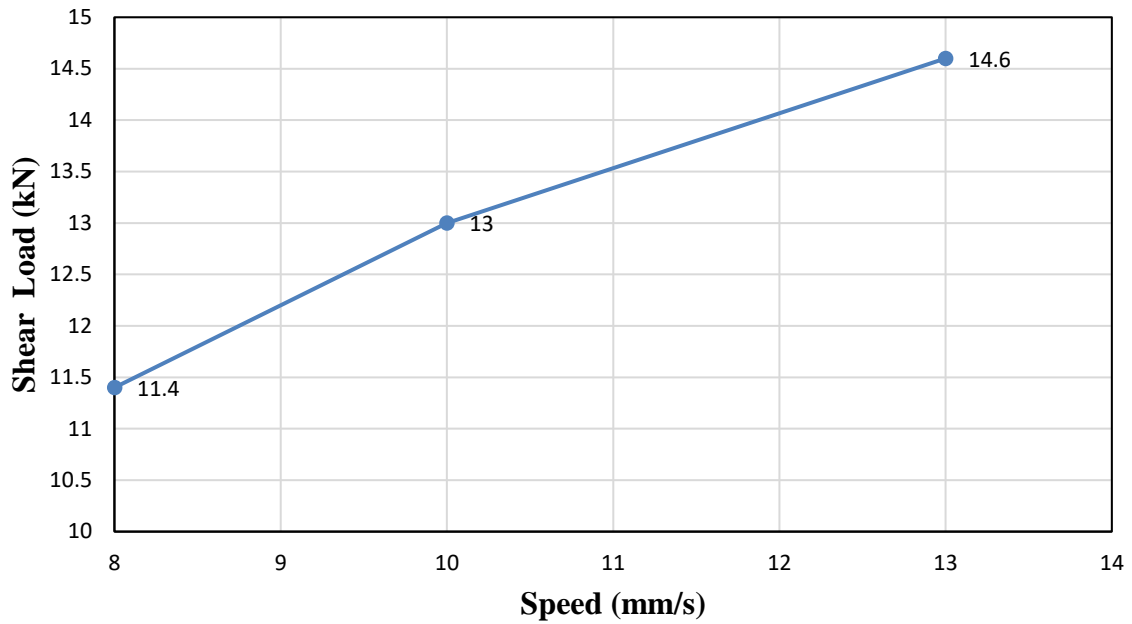
Fig.4.20 Effect of scan speed on shear load of specimen having copper cladding of 1- 4 layers.

4.7.2 Effect of hatch spacing on bond shear strength

For the samples fabricated with 0.25 mm scan spacing, there is a 0.60 % overlap between the subsequent scans, which resulted in more heat interaction, more cooling time and coarse grain structure. Samples fabricated with 0.25 mm hatch space have a maximum load of 11.3 kN whereas, for the 0.6mm hatch space, the maximum load was 25.5 kN due to 0% overlapping between subsequent layers.
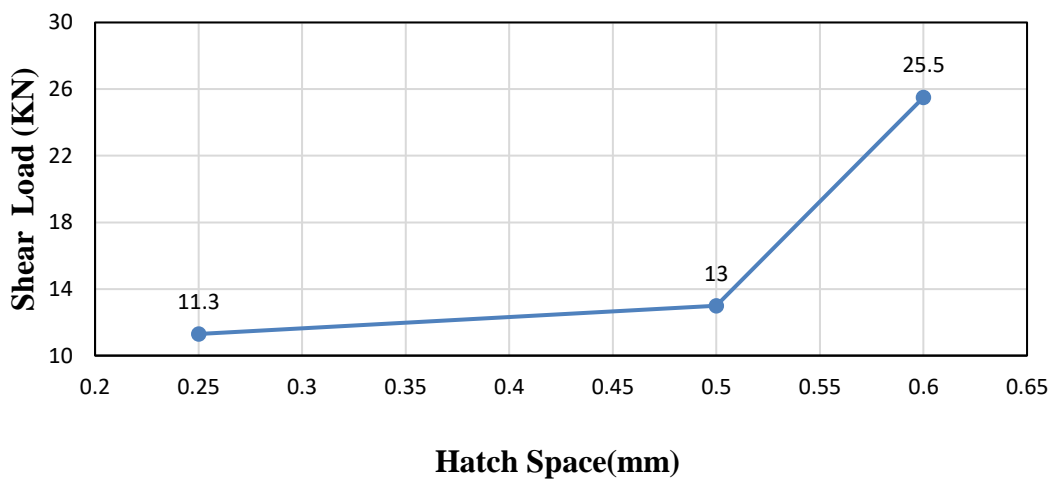
Fig.4.21 Effect of hatch space on shear load of specimen having copper cladding of 1- 4 layers.

4.7.3   Effect of scan strategies on bond shear strength

In bar graph fig.4.19   as observed the maximum load taken by the sample was fabricated with a horizontal scan strategy. This can be attributed to the rapid cooling rates, as also mentioned in the results of secondary dendritic arm spacing.
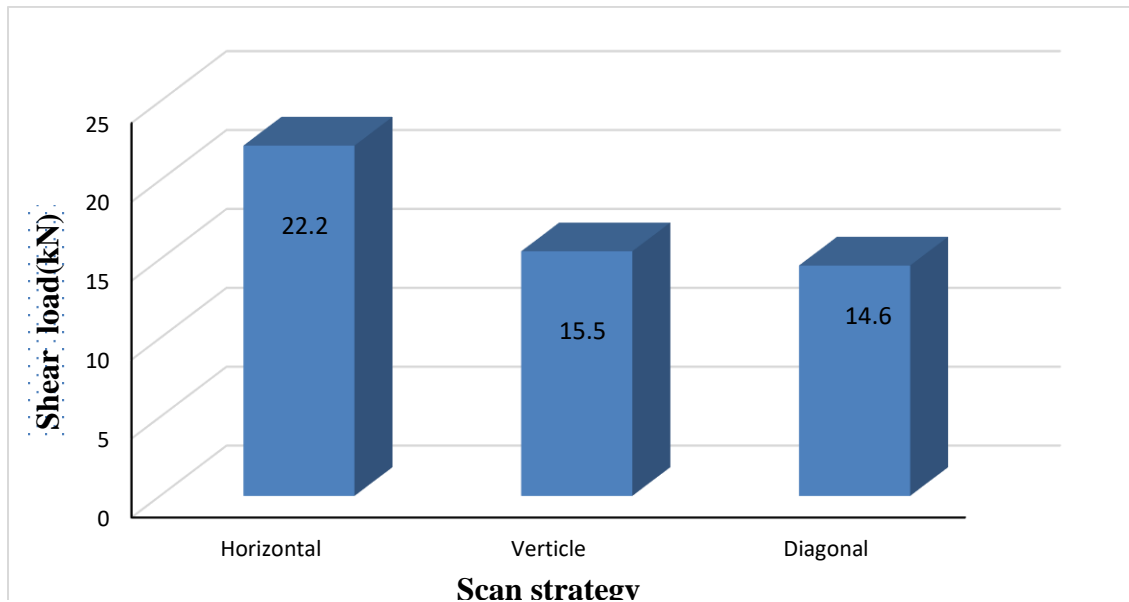
Fig.4.22 Effect of scan strategy on shear load of specimen having copper cladding of 1- 4 layers.

4.8   Secondary dendritic arm spacing (SDAS)

The secondary dendritic arm spacing of all the samples was measured with an image analyser software using the line intercept method. Optical images of the cladded sample show a highly dendritic structure. ImgaeJ software was used to measure the secondary dendritic arm spacing.
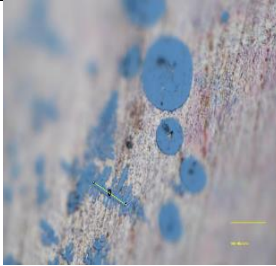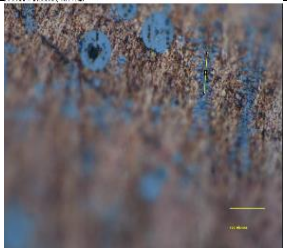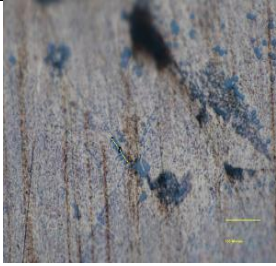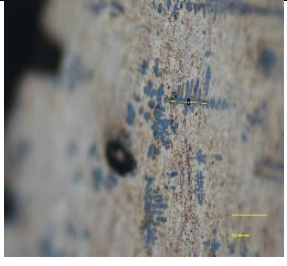
$$SDAS = \frac{Total\ length\ of\ primary\ dendrite\ under\ observation}{No.of\ secondary\ dendrites\ intercepted\ from\ primary\ dendrite}$$
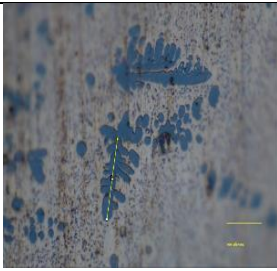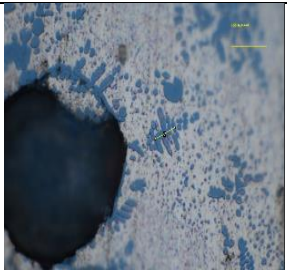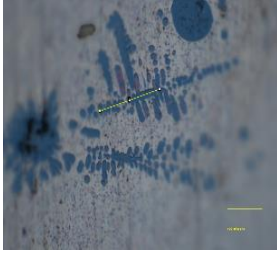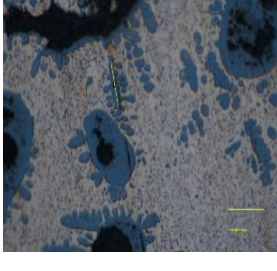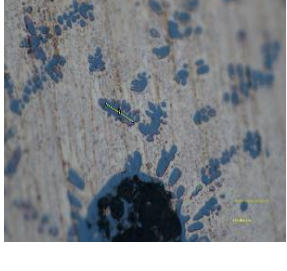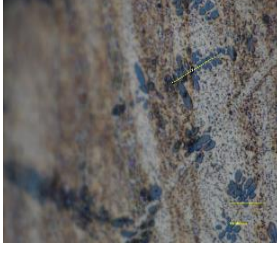
This formed dendritic structure confirms the liquid phase sintering mechanism. The melting point of steel is about 1520 °C whereas for copper it is 1083 °C. During cladding, the temperature increased above the melting point of both metals. Dendrites are formed due to the solidification that takes place over the temperature range and the segregation of alloying elements. Dendrite arm spacing depends on the cooling rates. Dendrite arm spacing decreases with an increase in the cooling rate. As the cooling rate decreases, more time is available for the diffusion of atoms of it to diffuse to a larger distance so the dendrite arm spacing increases. When power density is increased then it increases the cooling time resulting in more dendritic arm spacing. The same is the case for scan speed, for higher scan speed the

interaction time is low that is a low cooling time resulting in a smaller arm spacing. For the samples with 0.25 mm hatch space, as there is a 60 % overlap between subsequent scans, the interaction of heat will be more resulting in higher cooling time and higher arm spacing. In the case of the horizontal scan strategy, the dendritic arm spacing was found to be the least compared to vertical and diagonal scan strategies. The results showcasing the effect of the above parameters on dendritic arm spacing is shown in fig.
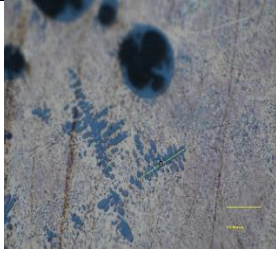
4.8.1 Micrographs for Secondary dendritic arm spacing

Table 4.5 Micrographs showing the dendritic microstructure for different laser processing parameters.

Parameters	Micrograph	Parameters	Micrograph
1)Power= 80W scan speed= 8mm/s hatch space=0.5mm scan strategy=H Layers=1 SDAS= 11.594 µm		2) Power= 100W scan speed= 8mm/s hatch space=0.5mm scan strategy=H Layers=1 SDAS= 9.806 µm	
3) Power= 80W scan speed= 8mm/s hatch space=0.5mm scan strategy=H Layers=2 SDAS= 13.647 µm		4) Power= 100W scan speed= 8mm/s hatch space=0.5mm scan strategy=H Layers=2 SDAS= 11.035 µm	
5) Power= 140W scan speed= 8mm/s hatch space=0.5mm scan strategy=H Layers=2 SDAS= 9.836 µm		6) Power= 80W scan speed= 8mm/s hatch space=0.5mm scan strategy=H Layers=3 SDAS= 9.194 µm	
7) Power= 100W scan speed= 8mm/s hatch space=0.5mm scan strategy=H Layers=3		8) Power= 140W scan speed= 8mm/s hatch space=0.5mm scan strategy=H Layers=3	

SDAS= 14.570 µm		SDAS= 13.318 µm	
9) Power= 80W scan speed= 8mm/s hatch space=0.5mm scan strategy=H Layers=4 SDAS= 30.476 µm		10) Power= 100W scan speed= 8mm/s hatch space=0.5mm scan strategy=H Layers=4 SDAS= 12.209 µm	
11) Power= 140W scan speed= 8mm/s hatch space=0.5mm scan strategy=H Layers=4 SDAS= 20.303 µm		12) Power= 140W scan speed= 10mm/s hatch space=0.25mm scan strategy=H Layers=3 SDAS= 15.598 µm	
13) Power= 140W scan speed= 10mm/s hatch space=0.5mm scan strategy=H Layers=3 SDAS= 25.456 µm		14) Power= 140W scan speed= 10mm/s hatch space=0.6mm scan strategy=H Layers=3 SDAS= 12.467 µm	
15) Power= 140W scan speed= 8mm/s hatch space=0.5mm scan strategy=H Layers=3 SDAS= 12.876 µm		16) Power= 140W scan speed= 10 mm/s hatch space=0.5mm scan strategy=H Layers=3 SDAS= 22.828 µm	
17) Power= 140W scan speed= 13mm/s hatch space=0.5mm scan strategy=H Layers=3 SDAS= 10.547 µm		18) Power= 170W scan speed= 10mm/s hatch space=0.5mm scan strategy=H Layers=3 SDAS= 8.905 µm	

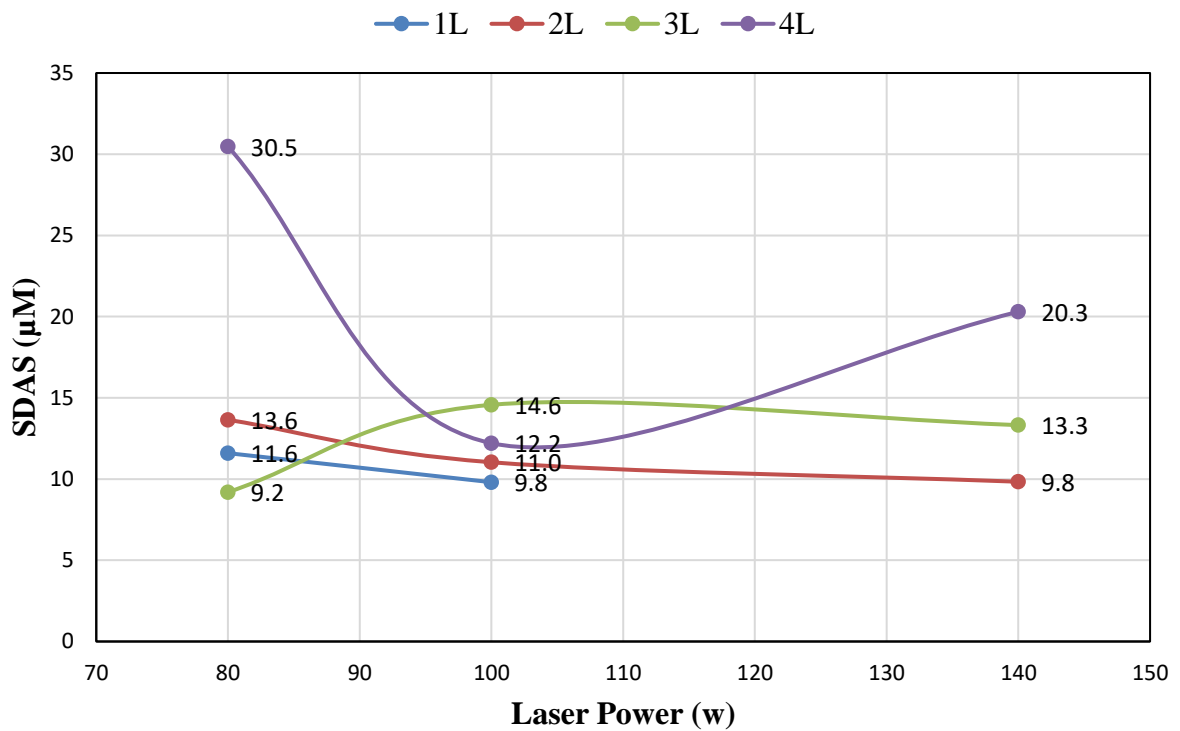| 19) Power= 170W scan speed= 10mm/s hatch space=0.5mm scan strategy=V Layers=3 SDAS= 10.234 µm		20) Power= 170W scan speed= 10mm/s hatch space=0.5mm scan strategy=D Layers=3 SDAS= 43.402 µm	

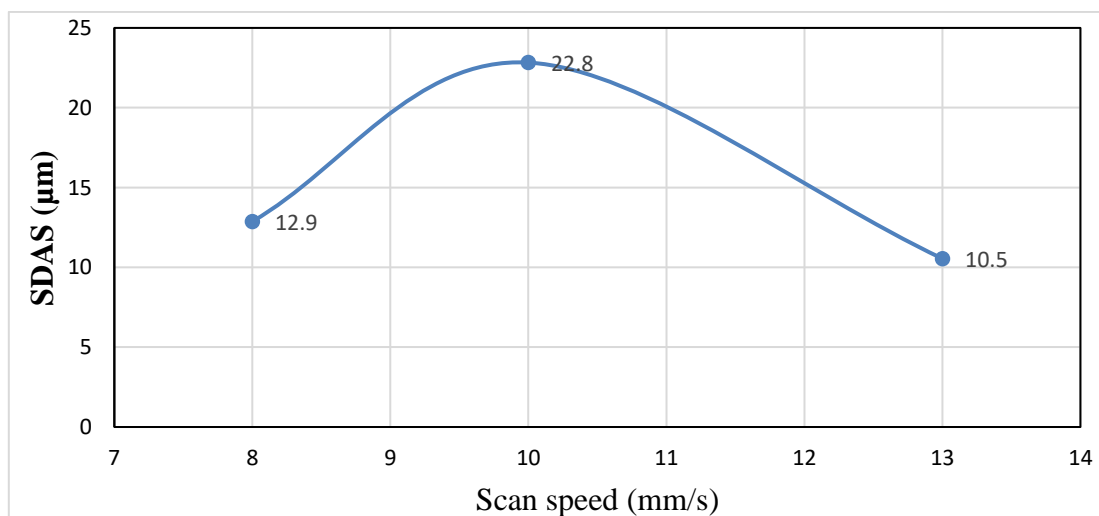Fig.4.23 Effect of laser power on SDAS of specimen having copper cladding of 1- 4 layers.

Fig.4.24 Effect of scan speed on SDAS of specimen having copper cladding of 1- 4 layers.
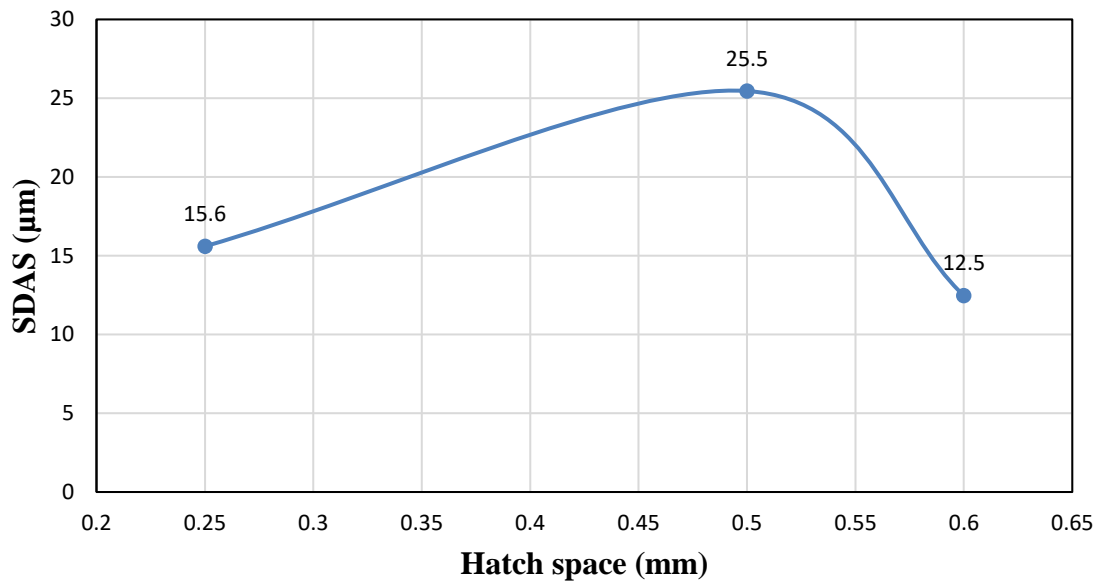
Fig.4.25 Effect of hatch space on SDAS of specimen having copper cladding of 1- 4 layers.
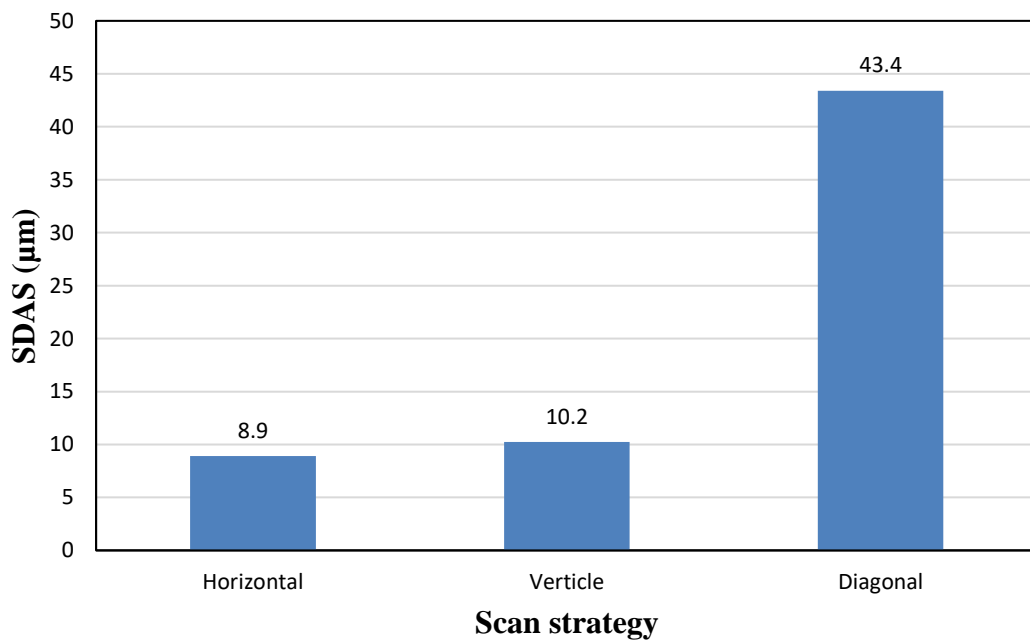

Fig.4.26 Effect of scan strategy   on SDAS of specimen having copper cladding of 1- 4 layers.

CHAPTER 5
CONCLUSIONS

1. Laser cladding of pure copper powder on a mild steel substrate using 3D printing setup with CO_2 laser was successfully completed. The modification of the copper pipe nozzle fixture so that argon is introduced well below the lower head, completely solved the problem of lens breaking.

2. Increasing the power from 80 W to 140 W, increased the maximum load from 6.2 kN to 21.3 kN during the bond shear strength test.

3. Increase in the secondary dendritic arm spacing was observed due to reduced cooling rate. It was increased when scan speed, hatch space were decreased and power was increased.

4. Microhardness results show some similar trend to bond shear strength results except for the samples made with different hatch spaces, this can be attributed to the experimentation mistakes.

5. Changing the scanning strategy also showed changes in their results, it was observed that the horizontal scan strategy has better results compared to the vertical and diagonal scan strategies. SDAS of 8.90 µm,10.23 µm, and 43.40 µm was observed for horizontal, vertical, and diagonal respectively. So, the presence of finer grains and higher cooling rates resulted in better properties of samples made with the horizontal scan strategy.

CHAPTER 6
REFERENCES

1. Lida Zhu a,*,1 , Pengsheng Xue a,1 , Qing Lan a , Guiru Meng a , Yuan Ren b , Zhichao Yang a , Peihua Xu a , Zhe Liu c – " **Recent research and development status of laser cladding: A review**".(2021)

2. Feifei Huang 1,2,* , Erju Liu 3,4 , Yi Qin 1 , Qingrui Wang 1 , Ying Jin 1,2,* , Lei Wen 1,2 and Hai Chang 1,2- "**A Study of Multi-Pass Laser-Cladding 2205 Duplex Stainless Steel Coating: Microstructure, Electrochemical Corrosion Behavior, and Wear-Resistance Properties "**(2022)

3. Feifei Huang 1,2,* , Erju Liu 3,4 , Yi Qin 1 , Qingrui Wang 1 , Ying Jin 1,2,* , Lei Wen 1,2 and Hai Chang 1,2- "**A Study of Multi-Pass Laser-Cladding 2205 Duplex Stainless Steel Coating: Microstructure, Electrochemical Corrosion Behavior, and Wear-Resistance Properties "**(2022)

4. Anas Ahmad Siddiqui * , Avanish Kumar Dubey**- "Recent trends in laser cladding and surface alloying"** (2021)….

5. Kohei Asano,1,2 Masahiro Tsukamoto,3 Yoshinori Funada,4 Yu Sakon,5 Nobuyuki Abe,3 Yuji Sato,3 Ritsuko Higashino,3 Masanori Sengoku,6 and Minoru Yoshida6 –**" Copper film formation on metal surfaces with 100 W blue direct diode laser system."**

6. K.R. Bakshi, A. V. Mulay **– "A Review on Selective Laser Sintering: A Rapid Prototyping Technology "** (2016)

7. Syed A.M. Tofail 1 , Elias P. Koumoulos 2 , Amit Bandyopadhyay 3 , Susmita Bose 3 , Lisa O'Donoghue 4,5 , Costas Charitidis**- "Additive manufacturing: scientific and technological challenges, market uptake and opportunities."** (2018)

8. Thomas Duda1 · L. Venkat Raghavan2 –**" 3D metal printing technology: the need to re-invent design practice "**(2017).

9. Catarina Valente, Teresa Morgado and Neeraj Sharma.- **"LASER Cladding—A Post Processing Technique for Coating, Repair and Re-manufacturing "**(2020)……

10. Syed A.M. Tofail 1 , Elias P. Koumoulos 2 , Amit Bandyopadhyay 3 , Susmita Bose 3 , Lisa O'Donoghue 4,5 , Costas Charitidis- **"Additive manufacturing: scientific and technological challenges, market uptake and opportunities."** (2018)

11. Thomas Duda1 · L. Venkat Raghavan2 - **3D metal printing technology: the need to re-invent design practice** (2017)

12. Anton Wiberg- **"Towards Design Automation for Additive Manufacturing A Multidisciplinary Optimization approach**".

13. Sining Pan, Gang Yu, **"Application of millisecond pulsed laser for thermal fatigue property evaluation"**, Optics and Laser Technology 99 (2018) 382–391.

14. William M. Steen · Jyotirmoy Mazumder **-" Laser Material Processing "**(4th Edition)

15. K. Shahzad et al., "**Additive manufacturing of alumina parts by indirect selective laser sintering and post processing, Journal of Materials Processing Technology** "(2013)

16. Lida Zhu a,*,1 , Pengsheng Xue a,1 , Qing Lan a , Guiru Meng a , Yuan Ren b , Zhichao Yang a , Peihua Xu a , Zhe Liu c –**" Recent research and development status of laser cladding: A review "**(2021).

17. S.K. Nayak, S.K. Mishra, C.P. Paul∗ , A.N. Jinoop, K.S. Bindra- **"Effect of energy density on laser powder bed fusion built single tracks and thin wall structures with 100 μm preplaced powder layer thickness"** (2020).

18. Essam R.I. Mahmoud a,⇑ , Sohaib Z. Khan a , Muhammad Ejaz b**- "Laser surface cladding of mild steel with 316L stainless steel for anti-corrosion applications "**(2020).

19. Vikas Kumar, Rahul Rakshit, Alok Kumar Das*- **"Mechanical and tribological performance of fiber laser cladded h-BN + SS316 composite on SS316 surface".**(2020).

20. Girish R. Desalea, C.P. Paul b, B.K. Gandhi c,∗, S.C. Jainc**- "Erosion wear behavior of laser clad surfaces of low carbon austenitic steel".**

21. Ravi Parekha,b,*, Ramesh Kumar Buddua , R.I. Patelb- **"Multiphysics simulation of laser cladding process to study the effect of process parameters on clad geometry"**.

22. Dongdong Gu*, Yifu Shen- **"Balling phenomena in direct laser sintering of stainless steel powder: Metallurgical mechanisms and control methods"**.

23. R. M. Mahamood1,2,3 and E. T. Akinlabi1**-" Effect Of The Scanning Speed Of Treatment On The Microstructure, Microhardness, Wear, And Corrosion Behavior Of Laser Metal-Deposited Ti–6al–4v/Tic Composite".**

24. Surinder Singha , Manoj Kumarb , Gurvinder Pal Singh Sodhia , Ramesh Kumar Budduc , Harpreet Singha,∗- **"Development of thick copper claddings on SS316L steel for In-vessel components of fusion reactors and copper-cast iron canisters"**.

25. ASM Handbook, Volume 10, Materials Characterization.

ACKNOWLEDGEMENT